CHARACTERIZATION OF BIOACTIVE SECONDARY METABOLITES FROM *PSEUDOMONAS AERUGINOSA* AND *PROROCENTRUM* SPECIES

Jennifer S. Williams

A Thesis Submitted to the
University of North Carolina at Wilmington in Partial Fulfillment
Of the Requirements for the Degree of
Master of Science

Center for Marine Science

University of North Carolina at Wilmington

2003

Approved by

Advisory Committee

_____ _____

_____
Chair

Accepted by

_____
Dean, Graduate School

TABLE OF CONTENTS

ABSTRACT

Environmental isolates of *Pseudomonas aeruginosa*, *Prorocentrum maculosum* and *Prorocentrum lima*, organisms that have an adverse impact on human health, were mined for bioactive secondary metabolites. Antibiotics isolated from the extracts of *P. aeruginosa* culture supernatant included pyoluteorin, phenazine-1-carboxamide, and five members of the 4-hydroxy-2-alkyl/alkenyl quinolines. Several diarrhetic shellfish poisons (DSPs) including okadaic acid, dinophysis toxin-1 and two new methyl derivatives of okadaic acid were isolated from the *Prorocentrum* species' cell-free culture media, while three diol esters of okadaic acid and one of DTX-1 were isolated from *P. lima* cell extracts. Isolation of the DSPs was facilitated by a new, efficient method designed during this investigation. Algal as well as bacterial isolates from this study were tested in a B-galactosidase bioassay designed to measure induction or inhibition of *P. aeruginosa* cell-to-cell signaling. The *P. aeruginosa* cell-signaling cascade was induced by select *P. aeruginosa* and *P. lima* extracts, however the presence of known *P. aeruginosa* autoinducers was not detected. OA and DTX-1 were found to have no significant impact on the cell-signaling cascade of the bioassay strain.

ACKNOWLEDGEMENTS

I would like to acknowledge the members of the Wright lab, both past and present, for their encouragement and help over the past two years. What a fantastic atmosphere! Anna, who taught me how to run my first LC column as well as countless other invaluable laboratory and life lessons… Laura, the after hours buddy… Amanda, quick to help out with the kids… Kristin, the smilin' undergrad with more lab experience than most of us, and always ready to share… Jermaine, who showed us that you really can leave the Wright lab with a degree and with a smile on your face… Lindsay and T. J., the new kids on the block… Eve, who spent hours culturing the microalgae used in this project… Dr. Wright, who encouraged me to pursue all my crazy ideas, spent endless hours discussing science and only told me to chill once…thank you!

I would also like to acknowledge others at UNCW's Center for Marine Science for their help in the completion of this project. Andrea, for both research and personal support… Sophie, for the many answers and ideas… Ashley, the fountain of knowledge on how to get your masters… Amanda, who spent hours culturing the bacteria used in this project… Dr. Baden and Dr. Sizemore, my committee members with so many thought provoking questions…thank you!

Finally, much gratitude goes to Dr. E. C. Pesci and Susan McKnight at the East Carolina University Brody School of Medicine for performing the cell-signaling assay used in this study and for their guidance in the realm of quorum sensing.

DEDICATION

I would like to dedicate this work to my family, David, Erika and Abby, mom and dad, for their help and support throughout this two-year roller coaster ride. Without each of you the process would have been neither possible, meaningful, nor enjoyable.

LIST OF TABLES

LIST OF FIGURES

INTRODUCTION

Bioactive Secondary Metabolites

Autoinducers, antibiotics and toxins were the focus of this search for bioactive secondary metabolites from organisms that have an adverse impact on human health. Discovery and characterization of bioactive secondary metabolites produced by these organisms could aid in the understanding of each organism's chemical advantages, possibly providing insight into ways of controlling these human pathogens. Revealing previously unidentified properties of known compounds in addition to the discovery of new bioactive compounds would aid in this endeavor. *Pseudomonas aeruginosa*, a bacterium, and *Prorocentrum maculosum* and *Prorocentrum lima*, two marine dinoflagellates, were chosen as representative organisms in this study.

Many invertebrates, plants and microorganisms, lacking the complex vertebrate immune system, produce secondary metabolites including those toxic to a variety of other organisms. Although not apparently essential in metabolic processes, these natural products appear to provide a mechanism of defense against invaders and confer a competitive advantage upon the producer (Wright, 2002). Although the ecological *raison d'être* of each secondary metabolite is ambiguous, laboratory bioassays have shown such compounds possess antibacterial (Hoyt and Sizemore, 1982), antifungal (Kerr, 2000), and antialgal properties (DellaGreca et al., 2003). Toxicity to higher organisms has been demonstrated in addition to other, more subtle bioactive properties including antilarval (Egan et al., 2001), antifeeding (Pawlik et al., 1987), and antifouling effects (Holmstrom et al., 2002; Henrikson and Pawlik, 1995).

Due to their bioactive properties, secondary metabolites have been traditionally mined from producing organisms for use in the pharmaceutical industry. Providing an assortment of diverse chemical structures selected over geologic time, "natural products are the most consistently successful source of drug leads" (Harvey, 2000), exhibiting a variety of mechanisms for killing pathogens. Pharmacologically significant antibacterial secondary metabolites such as penicillin and vancomycin inhibit bacterial cell wall synthesis (Rai et al., 2003; Allen and Nicas, 2003) while tetracycline and erythromycin inhibit bacterial protein synthesis (Metcalf et al., 2002; Schlunzen et al., 2003). Amphotericin B binds steroidal alcohols in the fungal membrane, demonstrating activity as a potent fungicide (Baran and Mazerski, 2002). Although receiving competition from combinatorial chemistry approaches, the search for bacteriocidal and fungicidal natural products continues to remain a viable source of drug leads, as only an estimated 10 % of the world's biodiversity has been explored (Harvey, 2000).

A more current approach to battling multi-drug resistant strains of pathogenic organisms such as *P. aeruginosa* has focused on disarmament of the organism rather than its complete eradication (Collier et al., 2002). Disruption of communication within a colony of *P. aeruginosa* by natural or synthetic cell signaling antagonists prevents the bacteria from producing virulence and survival factors, thereby precluding the pathogenicity of the organism (Calfee et al., 2001; Smith et al., 2003). Bacterial communication, also known as quorum sensing or cell-to-cell signaling, is a drug target that is gaining increased attention (Habeck, 2003).

Bacteria involved in quorum sensing produce small intercellular molecules, referred to as autoinducers, that when present in sufficient quantity regulate the

transcription of selected bacterial genes. An estimated 1 % to 4 % of the *P. aeruginosa* genome is controlled by autoinducers (McKnight et al., 2000). As cell density increases in a particular environment, autoinducer density increases and the binding of autoinducers to transcriptional regulator proteins is maximized. Autoinducers can regulate, at the transcription level, a suite of virulence factors (Van Delden and Iglewski, 1998), antibiotic production (Stead et al., 1996), biofilm formation (Van Delden and Iglewski, 1998), luminescence, and swarming motility (Rasmussen, 2000).

Limited examples of interspecies cell signaling are present in the current literature, including examples of both induction and inhibition of the cell signaling cascade. The cell signaling system of *Burkholderia cepacia*, often found co-infecting cystic fibrosis patient lungs in conjuction with *P. aeruginosa*, appears to be partially regulated by N-(3-oxododecanoyl)-L-homoserine lactone ($3OC_{12}HSL$; Figure 1a) and N-butyryl-L-homoserine lactone (C_4HSL; Figure 1b), two autoinducers synthesized by *P. aeruginosa*. In turn, the density dependent transcriptional regulator in *P. aeruginosa* is activated by N-octanoyl-L-homoserine lactone, an autoinducer produced by *B. cepacia* (Lewenza et al., 2002).

The disruption of bacterial cell signaling systems by secondary metabolites isolated from a marine macroalga has recently been demonstrated. Halogenated autoinducer analogs, 4-bromo-3-butyl-5-(dibromomethylene)-2(5H)-furanone (Figure 1c) and 4-bromo-5-(bromomethylene)-3-butyl-2(5H)-furanone (Figure 1d), produced by the seaweed *Delisea pulchra* appear to inhibit the swarming motility of *P. aeruginosa* and *Serratia* spp. by interfering with autoinducer binding (Rasmussen et al., 2000). Possibly

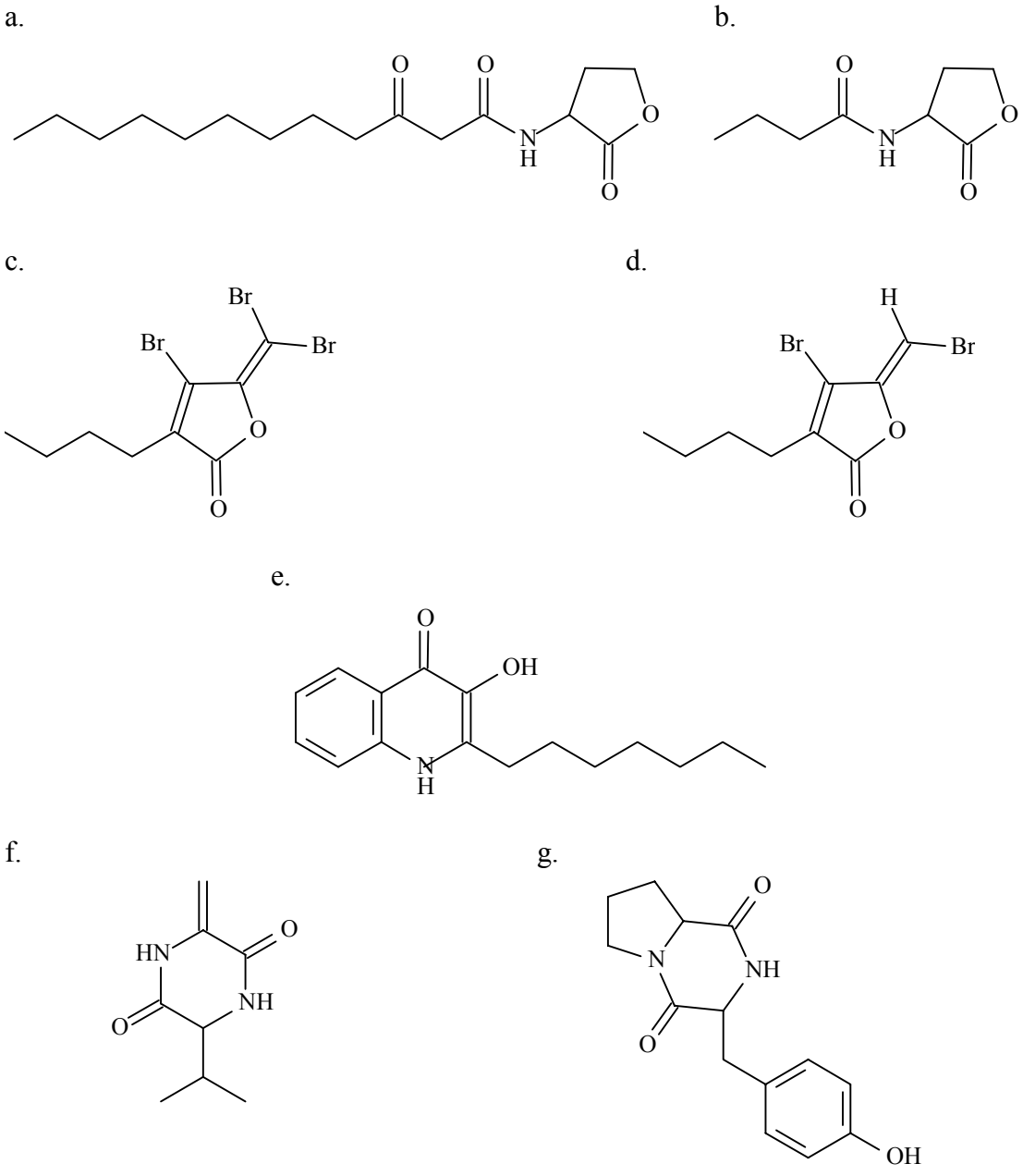

Figure 1. *P. aeruginosa* autoinducers and autoinducer antagonists.

a.) N-(3-oxododecanoyl)-L-homoserine lactone (autoinducer)
b.) N-butyryl-L-homoserine lactone (autoinducer)
c.) 4-bromo-3-butyl-5-(dibromomethylene)-2(5H)-furanone (antagonist)
d.) 4-bromo-5-(bromomethylene)-3-butyl-2(5H)-furanone (antagonist)
e.) 2-heptyl-3-hydroxy-4-quinolone (autoinducer)
f.) cyclo(ΔAla-L-Val) (autoinducer)
g.) cyclo (L-Pro-L-Tyr) (autoinducer)

produced as a defensive mechanism against bacterial fouling, the halogenated furanones comprise one group of natural products that inhibit autoinducer binding.

The discovery of new cell signaling inducers and inhibitors has wide reaching implications. Due to the lack of purified active transcriptional regulators, the testing of a suite of natural as well as synthetic autoinducer analogs is useful in gaining information on receptor-ligand interaction. Knowledge of the autoinducer binding site, a new drug target, would allow for specific synthesis of autoinducer analogs that would effectively compete with authentic autoinducer binding (Smith et al., 2003).

Pseudomonas aeruginosa

The gram-negative rod *P. aeruginosa* is an opportunistic pathogen of increasing significance in the realm of human health. Ubiquitous in the environment, *P. aeruginosa* flourishes in the individual with weakened immune system, current bacterial infection, or serious burn. Increasing resistance to multiple antibiotics makes *P. aeruginosa* virtually intractable once it colonizes the human host, and devastating effects can manifest (Van Delden and Iglewski, 1998). *P. aeruginosa* lung infections are the major cause of mortality in cystic fibrosis patients (Collier et al., 2002), with 49 % of cystic fibrosis children chronically infected with the pathogen (Baumann et al., 2003).

P. aeruginosa pathogenicity, resulting from the organism's ability to produce exotoxins harmful to humans, is regulated in part by cell-to-cell signaling (Smith and Inglewski, 2003). The survival of *P. aeruginosa* is also determined to a large extent by cell-to-cell signaling, which regulates the production of many of the bacteriocidal and fungicidal compounds synthesized by *P. aeruginosa,* thereby modulating the bacteria's mechanism of defense (Stead et al., 1996). Of the two known quorum sensing systems in

P. aeruginosa, the *las* system is activated by the autoinducer $3OC_{12}HSL$, while the *rhl* system is activated by C_4HSL (McKnight et al., 2000). Pesci et al. (1999) recently discovered an additional player in *P. aeruginosa* quorum sensing, the *Pseudomonas* quinolone signal (PQS) 2-heptyl-3-hydroxy-4-quinolone (Figure 1e), both a product of and regulator in quorum sensing. Cyclo(ΔAla-L-Val) (Figure 1f)and cyclo (L-Pro-L-Tyr) (Figure 1g), two diketopiperazines, have also been found to induce the quorum sensing of *P. aeruginosa* (Holden et al., 1999).

Upon reaching a quorum, *P. aeruginosa* produces a variety of antimicrobial compounds, thought to provide a competitive advantage as it vies for an attractive niche (Stead et al., 1996). Bacterial isolates from the rhizosphere of plants (Raaijmakers et al., 1997), lungs of cystic fibrosis patients (Michel-Briand and Baysee, 2002), and ears of otitis media sufferers (El-Samerraie et al., 1997) have demonstrated antibiotic activity against a variety of pathogenic organisms. Previously characterized antimicrobial compounds produced by *P. aeruginosa* include a group of peptides known as pyocins and an assortment of small heterocyclic compounds including the phenazines, quinolines and phenylpyrroles. Speculated to aid in *P. aeruginosa* colonization, these compounds destroy a range of other microorganisms through mechanisms ranging from DNA damage (Kerr, 2000) to cell depolarization (Michel-Briand and Baysee, 2002).

The pyocins are bacteriocins produced by *Pseudomonas* species. Bacteriocins were defined by Tagg et al., as plasmid-mediated proteinaceous compounds produced by bacteria that kill other, closely related bacteria (Klaenhammer, 1993; Contreras, 1997). Bacteriocins produced by *Pseudomonas* species are divided into R, F and S type pyocins. Both R and F type pyocins are large protein complexes that resemble bacteriophage tails,

while the S-type pyocin is a smaller, protease sensitive polypeptide pair. Of the two components of the S-type pyocin complex, one appears to confer immunity. The other component enters the iron-limited bacterial cell through a membrane ferripyoverdine receptor, exerting antibacterial activity by stimulating DNA breakdown (Parret and DeMot, 2002) and inhibiting phospholipid synthesis.

Gram negative bacteria are commonly dismissed as producing bacteriocins with very limited spectrums of activity (Mayr-Harting et al., 1972), thereby limiting potential commercial use and the number of current studies. A narrow activity spectrum is, however, irrelevant in determining a bacteriocin's commercial significance if toxigenic strains of pathogenic bacteria such as *P. aeruginosa* are within the spectrum. Hybridization of an S3-type pyocin with an S1-type pyocin resulted in an increased spectrum of activity against strains of *P. aeruginosa* inhabiting patient lungs (Michel-Briand and Baysee, 2002).

Significantly smaller antimicrobial compounds produced by *P. aeruginosa* are a diverse assemblage of heterocyclic compounds including the phenazines, quinolines and compounds containing a pyrrole moiety. The phenazines, produced by *Pseudomonas* species as well as *Streptomyces*, *Microbispora*, and *Sorangium* species, are pigments demonstrating broad-spectrum antimicrobial activity. With over fifty known structures, the phenazines include pyocyanin, the blue pigment characteristic of *P. aeruginosa* (Gerber, 1973).

Spanning the visible spectrum, phenazine pigments are differentiated based upon modifications to the phenazine heterocyclic ring system (Figure 2a) (Kerr, 2000). In addition to pyocyanin, 1-hydroxy-5-methylphenazine, *P. aeruginosa* is known to produce

other molecules in this class including phenazine-1-carboxylic acid (Tubermycin B), 1-hydroxyphenazine (Hemipyocyanin), and phenazine-1-carboxamide (Oxychlororaphine) (Gerber, 1973).

Induction of the phenazines has been shown to occur in response to the quorum signaling compound, L-N-(3-oxohexanoyl) homoserine lactone (Stead et al., 1996), with biosynthesis of the precursor, phenazine-1,6-dicarboxylic acid, occurring through the shikimic acid pathway (Kerr, 2000). Phenazine production has been directly correlated with *Pseudomonas* spp. antimicrobial activity (Li et al., 1995), survival and virulence. Proposed ecological functions of the phenazines include their action as antimicrobial agents, virulence factors (Kerr, 2000), and electron transport molecules (Hernandez and Newman, 2001).

The 4-hydroxy-2-alkylquinolines and their N-oxides comprise another class of heterocyclic molecules produced by *P. aeruginosa* that demonstrate antimicrobial properties against gram-positive bacteria including methicillin resistant *Staphylococcus aureus* (Taylor et al., 1995). Known as pseudans (Royt et al., 2001), this group of molecules is based on the 4-hydroxy-2-alkylquinoline structure (Figure 2b) and is differentiated based upon the size and degree of saturation of the alkyl chain, as well as the presence or absence of the N-oxide (Taylor et al., 1995). Pseudan IX, 4-hydroxy-2-nonylquinoline, and pseudan VII, 4-hydroxy-2-heptylquinoline, have recently been found to act as siderophores and reside in the cytoplasmic membrane of *P. aeruginosa* (Royt et al., 2001).

Pyoluteorin (Figure 2c) and pyrrolnitrin (Figure 2d) are two phenylpyrroles produced by *Pseudomonas* species that demonstrate broad-spectrum antimicrobial

a.

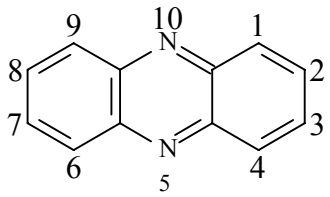

b.

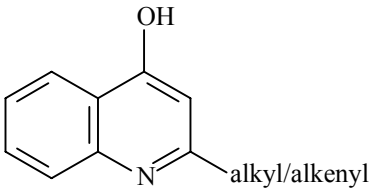

c.

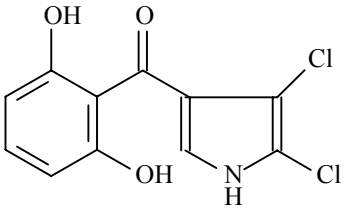

d.

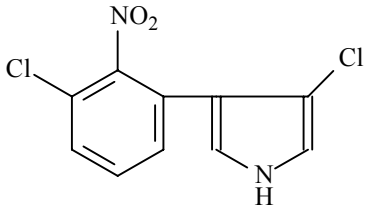

Figure 2. *P. aeruginosa* antibiotic secondary metabolites.
a.) phenazine
b.) 4-hydroxy-2-alkyl/alkenyl quinoline
c.) pyoluteorin
d.) pyrrolnitrin

activity, including activity against many plant root pathogens. Non-pathogenic *P. fluorescens* strains over-producing these antibiotics are currently being introduced as agricultural biocontrol agents (de Souza and Raaijmakers, 2003).

Production of the phenylpyrrole antifungal metabolites appears to be regulated by quorum sensing, as mutant strains exhibiting limited autoinducer production synthesize relatively few antifungal metabolites (Bloemberg and Lugtenberg, 2001). In addition to its production being regulated by quorum sensing, pyoluteorin also appears to act as a regulator in gene expression. The production of another autoinducer-regulated antifungal metabolite, 2, 4-diacetylphloroglucinol, appears to be repressed by pyoluteorin produced by the same organism (Schnider-Keel et al., 2000).

Prorocentrum species

Organisms of the genus *Prorocentrum* are benthic marine dinoflagellates, select species of which produce toxins known to be the causative agents of diarrhetic shellfish poisoning (DSP). Known as DSP toxins, okadaic acid (OA), dinophysis toxin-1 (DTX-1) and dinophysis toxin-2 (DTX-2) are hydrolysis products of larger sulfated diesters produced by *P. lima*, *P. concavum*, and *P. maculosum* (Macpherson et al., 2003; Hu et al., 1995). These toxins are concentrated in clams, mussels, and oysters as the shellfish filter feed on the toxin-producing dinoflagellates. The mechanism of action of DSP toxicity involves the inhibition of protein phosphatases I and IIa in eukaryotic organisms. Although the acute symptoms induced in mammals by DSP toxins are mild in comparison with marine toxins such as tetrodotoxin and brevetoxin, they are believed to be chronic tumor promotors (Landsburg et al., 1999; Baden et al., 1995).

OA (Figure 3a), DTX-1 (Figure 3b) and DTX-2 (Figure 3c) are cyclic polyether carboxylic acids with molecular weights of 804.5, 818.5 and 804.5, respectively, differing in structure by the quantity and location of methyl groups (Quilliam and Wright, 1995). Characteristic proton NMR signals of the DSP toxins include five olefinic proton signals, two of which exhibit doublet of doublet coupling, corresponding to the two protons on the central double bond (C-14 and C-15). The remaining three olefinic proton signals are singlets derived from protons located on C-9 and the carbon doubly bonded to C-25. Protons on carbons involved in the ether bonds of the DSP toxins exhibit chemical shifts in the 3-4 ppm range (Tachibana and Scheuer, 1981).

OA and DTX-1 parent compounds are the polar DTXs—large, nontoxic, sulfated diol esters of the DSP toxins biosynthesized by select *Prorocentrum* species, each containing two ester bonds (Wright et al., 1996). The sulfates DTX-4 (figure 4a), DTX-5a, and DTX-5b, were characterized previously (Hu et al., 1994) and are found solely within the cells. The DSP sulfated diesters undergo two enzyme-catalyzed hydrolysis steps resulting in the formation of the free acid. This process is believed to occur upon excretion of the sulfated diol ester from the organism or upon cell lysis, as cellular esterases residing within the cell membrane act to catalyze hydrolytic breakdown of the molecule (Hu et al., 1995).

The intermediate in the formation of a DSP toxin from its parent sulfated diol ester is referred to as an OA or DTX-1 diol ester, each containing a single ester bond. DTX-4, for example, is rapidly hydrolyzed in the presence of cellular esterases to form a C8 diol ester of OA (Figure 4b). More lipophilic than either okadaic acid or DTX-4, the

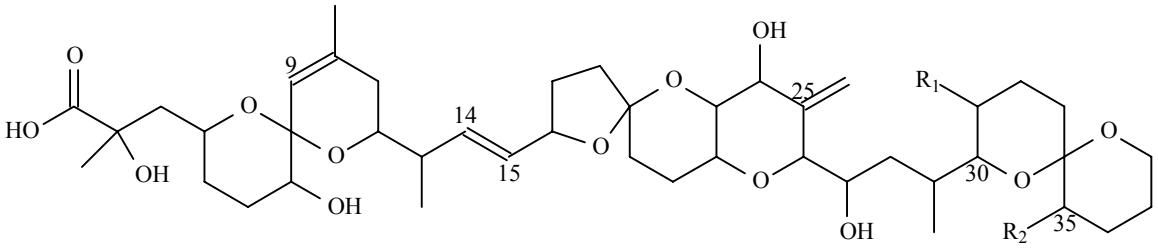

Compound	R_1	R_2
OA	CH_3	H
DTX-1	CH_3	CH_3
DTX-2	H	CH_3

Figure 3. Diarrhetic shelfish poisoning toxins.
a.) okadaic acid (OA)
b.) dinophysis toxin-1 (DTX-1)
c.) dinophysis toxin-2 (DTX-2)

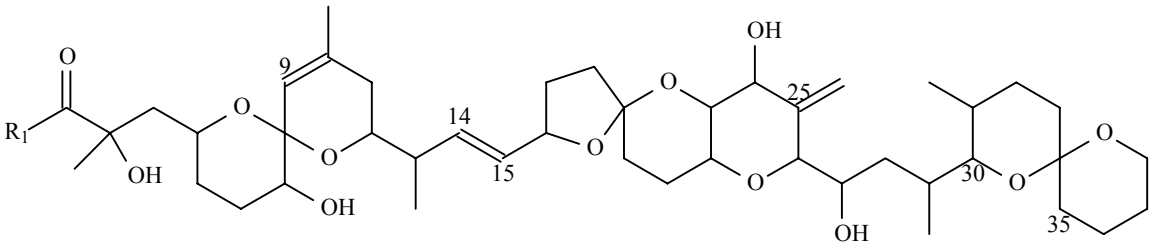

$\underline{R_1}$

a.

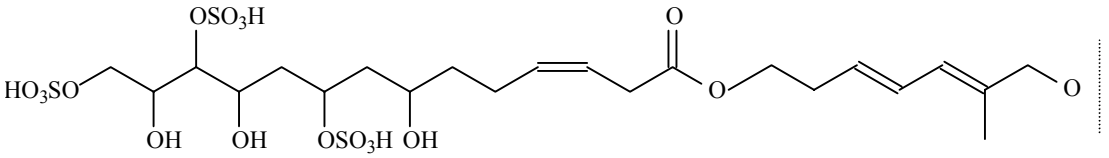

b.

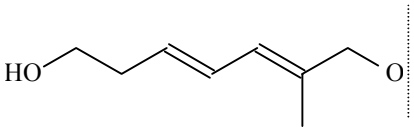

Figure 4. DSP parent compounds.
a.) DTX-4
b.) OA C_8 diol ester

OA-diol ester has demonstrated enhanced transfer across the cell membrane of the diatom *Thalassiosira weissflogii*, where it is hydrolyzed to OA *in situ* (Windust et al., 1997).

There has been much speculation on the initiation of bloom formation and toxin production in dinoflagellates. Intracellular and extracellular bacteria coexisting with dinoflagellates, both in vivo and in vitro, have been shown to have a symbiotic relationship with the dinoflagellate population, possibly initiating or contributing to toxin production (Prokic et al., 1998). Testing the effect of metabolites isolated from non-axenic cultures of dinoflagellates on a bacterial cell-signaling cascade could possibly reveal autoinducer molecules. These autoinducers would be of bacterial or dinoflagellate origin and could possibly control toxin production, bloom formation, or some other key aspect of the dinoflagellate population.

EXPERIMENTAL

Bioassays

Antibacterial and antifungal activities were detected with a disk diffusion bioassay and used in guiding fractionation. Mixtures and pure compounds to be tested were suspended in methanol and applied quantitatively to paper disks (0.55 cm) from Schleicher and Shuell. Test organisms used were the gram-positive bacteria *Bacillus subtilis* and *S. aureus*, the gram negative bacteria *Escherichia coli* and *P. aeruginosa*, and the yeast *Candida albicans*. These organisms were obtained from the Sizemore laboratory at the University of North Carolina at Wilmington and stored on nutrient agar slants at 4 °C until use. The assay was performed by inoculating nutrient broth with a test organism, incubating for 24 h, and applying the bacterial suspension to an agar plate with a sterile swab. The dried prepared disks, including a methanol control, were then placed on the swabbed plate using aseptic technique. The agar plate was incubated (37 °C; 24 h) prior to reading. Bacterial and fungal inhibition of simple mixtures and pure compounds was measured in activity units (AU), defined as the area of the cleared region in square millimeters divided by the mass of the applied material in milligrams.

Gamberdiscus toxicus, the mosquitofish, was the test organism utilized in the fish toxicity assay. Kept in a large saltwater tank prior to use, *G. toxicus* was prepared for bioassay by placing each fish in a beaker (50 ml) containing tank water (20 ml). To perform the assay, the test substance (0.5 mg) was dissolved in acetone (200 µl) and added to the fish water. Experimental fish were observed (24 h) and observations were noted regarding swimming speed, color change, loss of equilibrium, and mortality as compared to the control fish.

The Pesci lab in the Department of Microbiology and Immunology at the East Carolina University Brody School of Medicine performed the *P. aeruginosa* cell-signaling bioassay used in this study. The assay measured the production of B-galactosidase, an enzyme synthesized by *lacz* in the presence of an autoinducer. The assay was performed as described previously (Pesci et al., 1999).

Culture Methods

An environmental isolate of *P. aeruginosa* was cultured in the Sizemore lab at the University of North Carolina at Wilmington. Cultures were grown in media composed of proteose peptone (10 g), yeast extract (3 g), NaCl (23.4 g), MgSO4*7H2O (6.94 g), and KCl (0.75 g) per liter of water. Cultures were transferred from frozen stock to an agar plate and subsequently to media (20 ml). Following agitation (24 h) and incubation (36 °C), additional media was added to bring the total culture volume to 1L and incubation continued (48 h) prior to harvesting. Following incubation, the culture was centrifuged (15,000 x g) and the cell pellet discarded. The supernatant was saved for extraction.

Cells pelleted from non-axenic *P. maculosum* cultures (30 L) were obtained from the Tyndall lab in 2000 and frozen until extraction.

Non-axenic cultures of a Gulf of Mexico isolate of *P. lima* were obtained from the Tomas laboratory at the University of North Carolina at Wilmington. 250 ml of inoculum were used per liter of F/2 minus silica media, constituted in sterile seawater at a salinity of 36 ppt. Each liter of culture was grown in a Fernbach flask (4 L), cultured under constant light and temperature (22 °C) and gently swirled daily. The cultures were harvested following two months of growth.

Extraction Methods

Bacterial Isolates

Protein precipitation and solvent extraction were two techniques used to concentrate metabolites from *P. aeruginosa* culture supernatant. The initial fractionation of the *P. aeruginosa* culture supernatant (1 L) was attempted in order to optimize the precipitation of antimicrobial compounds. Ammonium sulfate was used to bring culture supernatant (1 L) to 20 % (152 g/L), 40 % (304 g/L), 60 % (456 g/L), and 80 % (608 g/L) saturation levels. A protein pellet was collected after centrifugation (15,000 x g) at each saturation level, fractions *Pa*1, *Pa*2, *Pa*3 and *Pa*4 respectively, and tested for antibacterial activity against *B. subtilis*, *P. aeruginosa,* and *E. coli* using a disk diffusion bioassay. The optimal saturation level was determined as 60% for the precipitation of antibiotic compounds, and ammonium sulfate (456 g/L) was slowly added to *P. aeruginosa* culture supernatant (9 L) with stirring. A protein pellet was collected after centrifugation and tested for antibacterial activity. All active material from protein precipitation was combined (*Pa*P).

P. aeruginosa culture supernatant (1 L) was extracted with ethyl acetate (500 ml x 2—*Pa*E) and subjected to antibacterial testing and TLC analysis.

Microalgal Isolates

Harvesting technique varied for each batch of *Prorocentrum* cells, but subsequent cell extraction and partitioning methods were identical. Following harvest, the cells were filtered, extracted with 80 % methanol (500 ml) and shaken against two volumes of hexane. The hexane layer was collected and the aqueous methanol layer dried and resuspended in 25 % methanol (500 ml). The aqueous methanol mixture was

subsequently shaken against two volumes of diethyl ether and butanol. The four fractions resulting from the partitioning were dried on a rotary evaporator and subjected to antibacterial, antifungal and ichthyotoxicity testing as well as TLC analysis.

The concentration of metabolites in *P. lima* cell free culture media was accomplished using two different techniques. The supernatant (January, 2003) remaining after continuous centrifuge (12 L) was concentrated on a conditioned C_{18} Sep Pak (60 ml) previously washed with DI water and subsequently eluted. The decanted culture media (May, 2003) (16 L) was filtered and the filtrate partitioned against ethyl acetate (4 L). *P. lima* cultures (42 L) harvested in July, 2003 were decanted and the decanted media filtered and partitioned against ethyl acetate (10.5 L). The cells were frozen in media (1 L), thawed, sonicated and left to stand overnight. The mixture was filtered and the filtrate concentrated on a conditioned C18 Sep Pack (60 ml).

Chromatography Methods

Thin layer chromatography (TLC) was performed on normal phase glass backed chromatography plates with fluorescent UV indicator. *P. aeruginosa* metabolites were chromatographed using mobile phase composed of chloroform-methanol (9 : 1). Plates were visualized using both short and long wavelength UV, sprayed with vanillin in dilute sulfuric acid in ethanol (vanillin 1) and heated.

The mobile phase used to separate the majority of *Prorocentrum* metabolites was a mixture of toluene-acetone-methanol (7.5 : 4 : 1). More polar compounds were chromatographed in ethyl acetate-isopropanol-water (8 : 3 : 1 or 8 : 5 : 3). Plates were visualized with both short and long wavelength UV and sprayed with vanillin (0.5 g) in

sulfuric acid-ethanol (4 : 1; 100 ml) (vanillin 2). Five minutes after spraying, plates were observed for color changes, heated and observed for additional color changes.

Stationary phases used in separation by low-pressure liquid chromatography were Sephadex LH-20 (25-100 μm) and Sephadex G-25 (size exclusion), Bakerbond C_{18} (40 μm) and Analtech C_{18} (35-75 μm) (reverse phase), EM Science Silica Gel 60 (0.040-0.063 mm) (normal phase) and Amberlite XAD2 (ion exchange). High performance liquid chromatography (HPLC) stationary phases used were Vydac C_{18} , Zorbax C_{18}, Phenomenex Luna C_{18}, and Phenomenex Luna Phenyl-hexyl. Solvents used were HPLC grade methanol, ethanol, acetonitrile, hexane, methylene chloride, chloroform, ethyl acetate, and trifluoroacetic acid (TFA) purchased from Fisher Scientific. Water was purified by a Labconco Water Pro Plus water deionization system.

Analytical Methods

Analytical HPLC with ultraviolet diode array detection (UVDAD) was performed on a Hewlett Packard Series 1100 HPLC.

Liquid chromatography/mass spectrometry (LC/MS) was performed on a hybrid Hewlett Packard Series1100 HPLC / Waters Micromass ZQ with electrospray ionization. MS conditions for all experiments alternated between electrospray positive and negative for a series of cone voltages (25, 50, 75, 100, and 125 V) (capillary 3.50 kV; extractor 5 V; RF lens 0.5 V; source temperature 125 °C; desolvation temperature 350 °C; desolvation gas flow 350 L/h; cone gas flow 50 L/h).

Nuclear magnetic resonance (NMR) experiments were performed on a Bruker 400MHz NMR and a 500MHz NMR.

Bioassay, TLC and NMR-guided Fractionation

P. aeruginosa

The active protein pellet derived from *P. aeruginosa* culture supernatant (*Pa*P—10 L) was divided into two parts. A portion (20 %) of the protein pellet (*Pa*1P) was used in an initial fractionation procedure to correlate bioactivity with TLC. The remaining pellet from eight liters of *P. aeruginosa* culture supernatant (*Pa*2P) was stored for later bulk fractionation.

TLC was performed in conjunction with antibacterial bioassays at each step of the fractionation of *Pa*1P (Figure 5). Fractionation began with an Amberlite XAD2 column (6 x 10.5 cm) washed with 0.1 % TFA. The precipitate was suspended in 0.1 % TFA (4 ml), applied to the column and eluted with one column volume each of 0 %, 25 %, 50 % 75 %, and 100 % ethanol / 0.1 % TFA. Antibacterial fractions were combined and TLC performed.

The active mixture eluted with 0.1 % TFA from the Amberlite column (*Pa*1P1) was dissolved in 0.1 % TFA (1 ml) and applied to a Sephadex G-25 column (2.5 x 16 cm) previously washed with 0.1 % TFA. The mixture was eluted with two column volumes of 0.1 % TFA, and fractions were collected. Each fraction underwent subsequent antibacterial testing and TLC.

Active fractions from the Sephadex column were combined (*Pa*1P1-2), dried onto Analtech C18 packing, and applied to a washed Analtech C_{18} column (1 x 13.5 cm). The mixture was eluted from the column using a gradient of acetonitrile (5 to 95 %) in 0.1 % TFA. Active fractions were combined and TLC performed.

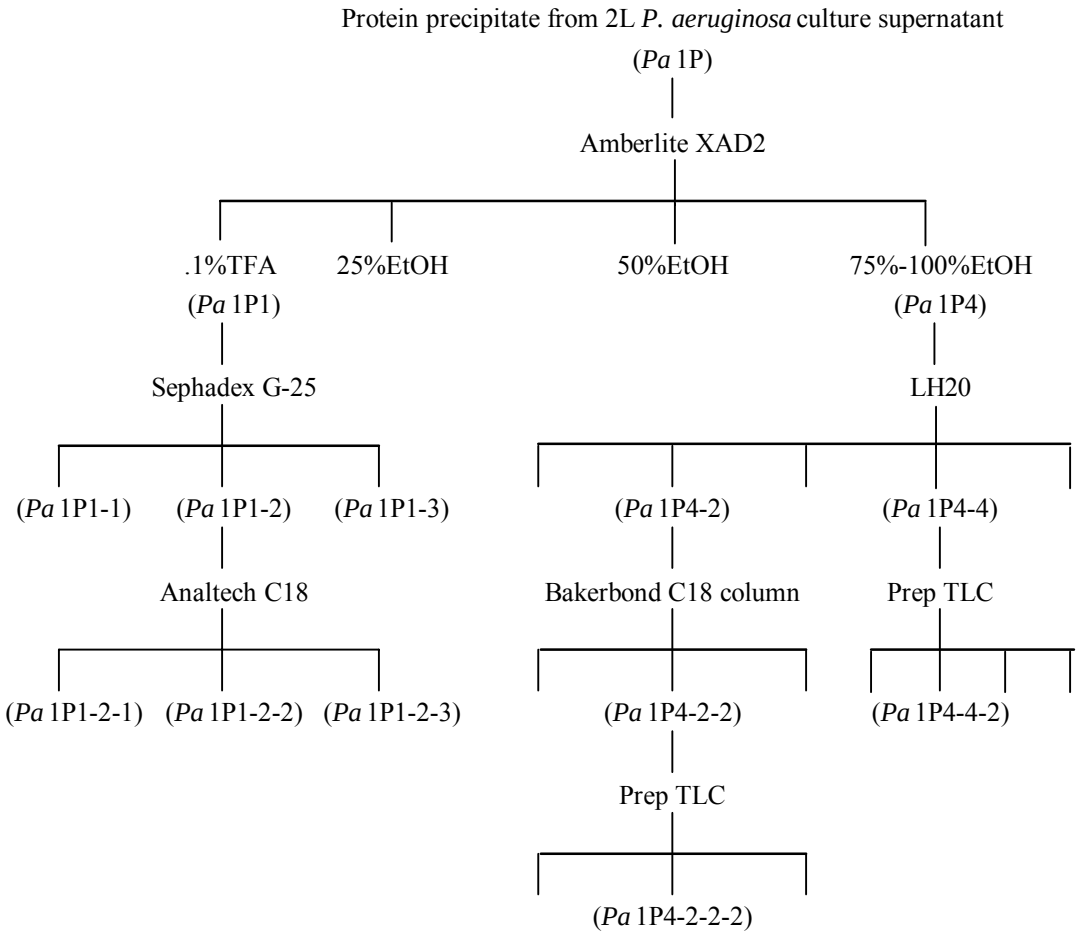

Figure 5. *Pa*1P fractionation scheme.

Active fractions from the Analtech column (*Pa*1P1-2-1) were dried onto Bakerbond C_{18} packing and applied to a washed column (1.2 x 4.5 cm) of the same material. Elution was performed with one column volume of 2, 4, 6, 8, 10, 20, 40, 70, and 100 % acetonitrile in 0.1 % TFA. Antibacterial activity was not detected in the fractions resulting from this step.

A second antibacterial mixture (*Pa*1P4), eluted from the original Amberlite column with 75 % to 100 % ethanol / 0.1 % TFA, was subjected to further fractionation. The mixture was suspended in methanol / 0.1 % TFA (0.5 ml), applied to an LH-20 column (1.2 x 9.5 cm), and eluted with two column volumes of methanol / 0.1 % TFA. Two separate sets of active fractions were combined based on bioassay and TLC.

The early eluting set of active fractions from the LH-20 column (*Pa*1P4-2) was dried onto Bakerbond C_{18} packing and applied to a column of the same material (1.2 x 4.5 cm), previously washed with 5 % acetonitrile / 0.1 % TFA. The column was eluted with an acetonitrile gradient in 0.1 % TFA. Fractions were combined based on antibacterial activity.

Preparative TLC was performed on the combined active fractions from the Bakerbond column (*Pa*1P4-2-2). TLC plates were washed with chloroform-methanol (9 : 1) and dried prior to application of the mixture. Plates were run in chloroform-methanol (9 : 1), allowed to dry, and visualized with UV light. The plates were divided into bands (approximately 1 cm), taking care to isolate UV active spots within individual bands. The bands were scraped and silica scrapings eluted with methanol. Each methanol mixture was then filtered with Millipore filters (5μm), dried and tested for antibacterial

activity. *Pa*1P4-2-2-2 correlated with bioactivity against *B. subtilis* and appeared purple under short wave UV light (R_f = 0.55; 9 : 1 chloroform-methanol).

This preparatory TLC procedure was repeated on the late eluting set of fractions from the LH-20 column (*Pa*1P4-4). *Pa*1P4-4-2 correlated with antibacterial activity against *B. subtilis*, *E. coli*, and *P. aeruginosa*. This spot (R_f = 0.357; 9 : 1 chloroform-methanol) was light yellow in color, UV active, and stained pink with vanillin 1.

In order to gain sufficient pure material for chemical analysis, fractionation of the remaining *P. aeruginosa* protein precipitate (*Pa*2P) was undertaken (Figure 6). *Pa*2P, derived from the protein precipitation of culture supernatant (8 L), was divided into two equal weights and applied separately to the same Amberlite XAD2 column used in the *Pa*1P fractionation. Fractions were lyophilized prior to antibacterial testing.

Substances eluting from 75 % to 100 % ethanol / 0.1%TFA (*Pa*2P4) from each Amberlite column were combined, divided into four equal weights, suspended in methanol / 0.1 % TFA (0.5 ml), and applied individually to an LH-20 column (1.2 x 15 cm). Each column was eluted with two column volumes of methanol / 0.1 % TFA. Fractions were combined based on TLC and lyophilized prior to bioassay. Two sets of active fractions resulted. The early eluting antibacterial fractions from the LH-20 column (*Pa*2P4-2) were dried onto Analtech C_{18} packing and applied to an Analtech column (1 x 7 cm). The column was washed with 5 % acetonitrile / 0.1 % TFA and eluted with an acetonitrile / 0.1 % TFA gradient (5-95 %). Fractions were combined based on TLC, lyophilized and tested for antibacterial activity.

Analytical HPLC was performed on the combined, active fractions from the Analtech column (*Pa*2P4-2-2). The mixture was suspended in 45 % acetonitrile / 0.1 %

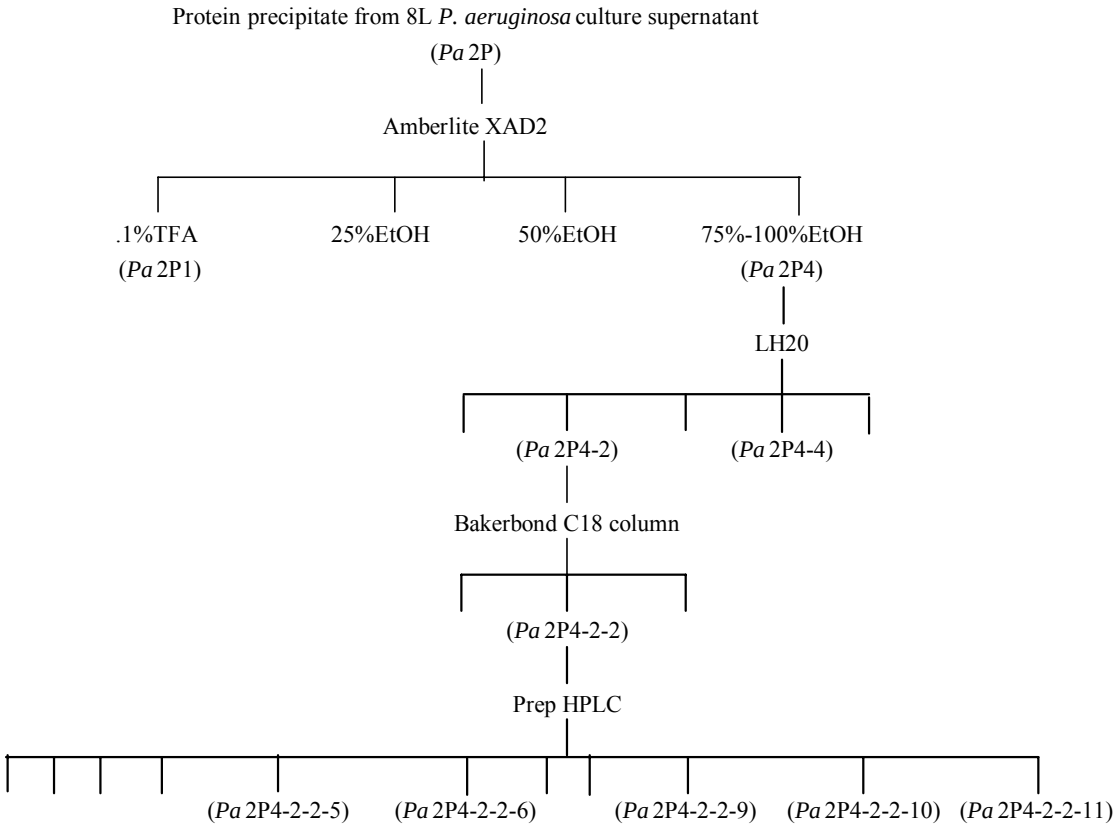

Figure 6. *Pa*2P fractionation scheme.

TFA and an aliquot (15 µl) injected onto a Vydac C_{18} column (4.6 x 250 mm; elution 45 % acetonitrile / 0.1 % TFA; flow rate 1.4 ml/min). Preparative HPLC was subsequently performed using a Vydac C_{18} column (9.4 x 250 mm; elution 45 % acetonitrile / 0.1 % TFA; flow rate 2.5 ml/min; detection 210 and 240 nm). Eleven peaks were collected, lyophilized, and tested for antibacterial activity.

The five bioactive compounds obtained by preparative HPLC (*Pa*2P4-2-2-5, 6, 9, 10, and 11), were dissolved in deuterated methanol and analyzed by ^{1}H NMR. LC/MS was performed on the individual compounds, using a Zorbax C_{18} column (2 x 50 mm; elution 45 % acetonitrile / 0.1 % TFA; flow rate 0.21 ml/min). Each of the five compounds was tested in a *P. aeruginosa* cell-signaling assay (see Table 1). Additional biological and analytical data for each compound are reported below.

*Pa*2P4-2-2-5 (4.4 mg): UV λ max (acetonitrile / 0.1 % TFA) 230, 300 nm; inhibition (*B. subtilis*) 315 AU; esims $[MH]^+$ 244, $[MH-85]^+$ 159; ^{1}H NMR (400MHz) in CD_3OD δ 8.28 (1H, d, J = 8.20 Hz), 7.82 (1H, t, J = 8.02 Hz), 7.74 (1H, d, J = 8.41 Hz), 7.54 (1H, t, J = 7.72 Hz), 6.55 (1H, s), 2.85 (2H, t, J = 7.79 Hz), 1.81 (2H, p, J = 7.85 Hz), 1.24-1.41 (8H, m), 0.89 (3H, t, J = 6.72 Hz).

*Pa*2P4-2-2-6 (4.0 mg): UV λ max (acetonitrile / 0.1%TFA) 235, 305nm; inhibition (*B. subtilis*) 395 AU; esims $[MH]^+$ 260, $[MH-16]^+$ 244, $[MH-16-85]^+$ 159; ^{1}H NMR (400 MHz) in CD_3OD δ 8.30 (1H, d, J = 7.93 Hz), 8.17 (1H, d, J = 8.59 Hz), 7.89 (1H, t, 7.78 Hz), 7.58 (1H, t, J = 7.63 Hz), 6.50 (1H, s), 3.00 (2H, m), 1.81 (2H, p, J =7.73 Hz), 1.26-1.46 (8H, m), 0.91 (3H, t, J =6.70 Hz).

*Pa*2P4-2-2-9 (4.2 mg): UV λ max (acetonitrile / 0.1 % TFA) 260, 320 nm; inhibition (*B. subtilis*) 195 AU; esims $[MH]^+$ 270, $[MH-85]^+$ 185, $[MH-85-26]^+$ 159; ^{1}H

Sample Name	Mass (ug)	B-galactosidase Activity (Miller Units)	
		Sample	Control
Pa P4-2-2-5	30	304	405
Pa P4-2-2-6	30	535	405
Pa P4-2-2-9	30	377	405
Pa P4-2-2-10	30	1180	405
Pa P4-2-2-11	30	376	405
Pa E2-2	30	471	405
Pa E2-2-3	10	456	313
	40	450	274
Pa E2-2-4	10	319	313
	40	288	274
Pa2P4-2-2-10-1	10	357	313
	40	326	274
Pa2P4-2-2-10-2	10	383	313
	40	620	274
Pa2P4-2-2-10-3	10	321	313
	40	254	274
Pa2P4-2-2-10-2-1	10	379	306
	10	338	306
	40	422	318
	40	453	318
	40	300	276
	40	366	313
	40	394	328
Pa2P4-2-2-10-2-2	10	329	306
	40	378	318

Table 1. Cell-signaling results for *P. aeruginosa* metabolites.

NMR (400 MHz) in CD_3OD δ 8.25 (1H, d, J = 8.43 Hz), 7.79 (1H, t, J = 8.21 Hz), 7.75 (1H, d, J = 8.00 Hz), 7.50 (1H, t, J = 6.38 Hz), 6.97 (1H, dt, J = 16.30 Hz, 7.78 Hz), 6.67 (1H, s), 6.48 (1H, d, J = 16.01 Hz), 2.39 (2H, q, J = 7.15 Hz), 1.58 (2H, p, J = 7.36 Hz), 1.26-1.39 (8H, m), 0.92 (3H, t, J = 6.72 Hz).

*Pa*2P4-2-2-10 (7.9 mg): UV λ max (acetonitrile / 0.1 % TFA) 225, 300 nm; inhibition (*B. subtilis*) 250 AU; esims $[MH]^+$ 272, $[MH-113]^+$ 159;^{1}H NMR (400 MHz) in CD_3OD δ 8.30 (1H, d, J = 7.96 Hz), 7.84 (1H, t, J = 7.26 Hz), 7.77 (1H, d, J = 8.18 Hz), 7.57 (1H, t, J=7.31 Hz), 6.62 (1H, s), 2.87 (2H, t, J = 7.33 Hz), 1.81 (2H, p, J = 6.14 Hz), 1.22-1.41 (12H, m), 0.90 (3H, t, J = 6.23 Hz).

*Pa*2P4-2-2-11 (6.5mg): UV λ max (acetonitrile / 0.1 % TFA) 230, 305nm; inhibition (*B. subtilis*) 141 AU; esims $[MH]^+$ 288, $[MH-16]^+$ 272, $[MH-16-113]^+$ 159;^{1}H NMR (400 MHz) in CD_3OD δ 8.30 (1H, d, J = 8.11 Hz), 8.16 (1H, d, J = 8.56 Hz), 7.91 (1H, t, J =7.78 Hz), 7.59 (1H, t, J = 7.01 Hz), 6.53 (1H, s), 3.01 (2H, m), 1.82 (2H, p, J = 7.73 Hz), 1.24-1.49 (12H, m), 1.91 (3H, t, J = 6.73 Hz).

*Pa*2P4-2-2-10 was subjected to further cleanup. After elution from an LH-20 column (1 x 10 cm), *Pa*2P4-2-2-10-1, 2, and 3 were tested in the cell signaling bioassay (see Table 1) and underwent TLC analysis. ^{1}H NMR was performed on *Pa*2P4-2-2-10-2. Final purification of *Pa*2P4-2-2-10-2 was achieved using an additional HPLC procedure using a Phenomenex Luna Phenyl-hexyl column (4.6 x 250 mm; elution 45 % acetonitrile / 0.1 % TFA; flow rate 0.4 ml/min). Two compounds, *Pa*2P4-2-2-10-2-1 ($[MH]^+$=272) and *Pa*2P4-2-2-10-2-2 ($[MH]^+$=286) were collected and tested in the cell signaling bioassay (see Table 1). ^{13}C NMR results for *Pa*2P4-2-2-10-2-1 are shown below.

*Pa*2P4-2-2-10-2-1: ^{13}C NMR (500 MHz) in CD_3OD δ 133.2, 132.0, 124.5, 123.6, 117.6, 107.4, 33.6, 31.6, 29.1, 28.9, 28.8, 28.8, 28.7, 22.3, 13.0.

In an attempt to retrieve a larger mass of the LH-20 late eluting material from the *P. aeruginosa* culture supernatant (*Pa*2P4-4), an alternate extraction and purification technique was utilized (Figure 7). Culture supernatant (1 L) was shaken against ethyl acetate (500 ml). The three phases formed, organic, aqueous and emulsion, were separated and the emulsion subsequently shaken against fresh ethyl acetate (200 ml). The two ethyl acetate extracts (*Pa*E) were combined, dried and subjected to antibacterial testing and TLC analysis. Material contained in the ethyl acetate partition was applied to a Silica Sep pack (60 ml; elution 70 %, 50 %, and 30 % hexane in chloroform; 100 % chloroform; 1, 2, 5, 10, and 50 % methanol in chloroform). Antibacterial bioassay and TLC were performed on the fractions.

The combination of fractions containing the desired TLC spot (*Pa*E2) was suspended in methanol and applied to an LH-20 column (1.2 x 10 ml). The column was eluted with two column volumes of methanol and fractions with desired TLC spot combined.

Analytical HPLC was performed on the late eluting bioactive mixture from the LH20 column (*Pa*E2-4). The mixture was suspended in 20 % acetonitrile / 0.1 % TFA and an aliquot injected onto a Zorbax C_{18} column (2 x 50 mm; elution 20 % acetonitrile / 0.1 % TFA; flow rate 0.21 ml/min; UV monitoring). LC/MS was performed on the mixture, using a Zorbax C_{18} column (2 x 50 mm; elution 20% acetonitrile / 0.1 % TFA; flow rate 0.21 ml/min).

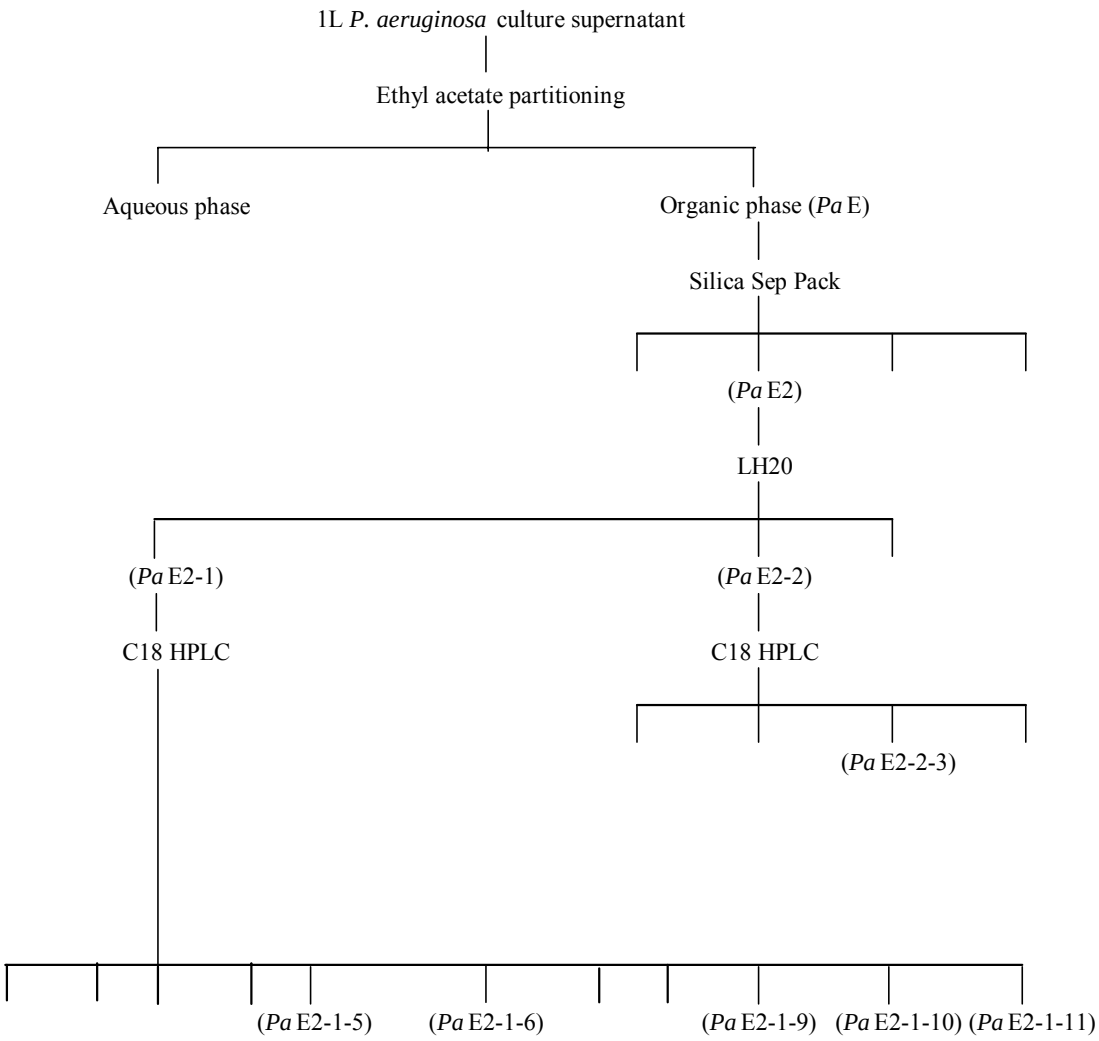

Figure 7. *Pa*E fractionation scheme.

The mixture was separated using a Vydac C_{18} column (9.4 x 250 mm; elution 30% acetonitrile / water; flow rate 2.5 ml/min). Antibacterial assays against *B. subtilis*, *E. coli*, *C. albicans*, *S. aureus*, and *P. aeruginosa* (parent and stock strains) were performed on the isolated compounds. 1D and 2D NMR data were obtained on the compound exhibiting antibacterial activity (*Pa*E2-2-3). *Pa*E2-2-3 and *Pa*E2-2-4 were tested in the cell signaling bioassay (see Table 1). Additional biological and analytical data for *Pa*E2-2-3 and *Pa*E2-2-4 are reported below.

*Pa*E2-2-3 (3.2 mg): UV λ max (acetonitrile / 0.1 % TFA) 206, 258, 310 nm; inhibition (*B. subtilis*) 6359 AU, (*E. coli*) 5024 AU, (stock *P. aeruginosa*) 7850 AU, (*S. aureus*) 9499 AU, (parent *P. aeruginosa*) 0 AU, (*C. albicans*) 0 AU; esims $[MH]^+$ 272, 274, 278 (9 : 6 : 1), $[MH-135]^+$ 137; ^1H NMR (400 MHz) in CD_3OD δ 7.08 (1H, t, J = 8.2 Hz), 6.55 (1H, s), 6.37 (2H, d, J = 8.2 Hz) ^{13}C NMR (400 MHz) in CD_3OD δ 185.7, 163.2, 160.2, 158.1, 145.7, 132.8, 132.3, 121.7, 119.0, 115.1, 111.9, 108.0.

*Pa*E2-2-4 (0.4 mg): UV λ max (acetonitrile / 0.1 % TFA) 204, 248, 368 nm; esims $[MH]^+$ 224, $[MH-17]^+$ 207, $[MH-45]^+$ 179; ^1H NMR (400 MHz) in CD_3OD δ 8.86 (1H, d, J = 7.2 Hz), 8.46 (1H, d, J = 8.6 Hz), 8.36 (1H, d, J = 9.6), 8.30 (1H, d, J = 9.9), 7.94 – 8.07 (3H, m).

P. maculosum

Cells from *P. maculosum* (30 L) were harvested in 2000 by centrifugation and the cell pellet frozen until extraction. Cell filtration, extraction and partitioning were performed as described previously and TLC performed on the extracts. The hexane extract (*Pm*H) was dried, resuspended in 50 % methanol (100 ml) and repeatedly partitioned against hexane (4 x 100 ml). The fractionation scheme for the *P. maculosum*

hexane extract is shown in Figure 8. The aqueous methanol partition (*Pm*HM) was dried, suspended in methanol (0.5 ml), applied to a prewashed LH-20 column (1 x 10 cm) and eluted with two column volumes of methanol. Fractions were combined based upon TLC. *Pm*HM2 was visualized on TLC with heat as a mixture of baseline and mid-plate pink staining spots. This mixture was dried onto silica packing, applied to a silica column (1 x 10 cm) and eluted successively with one column volume each of 5, 10, 20, 30, 40, and 50 % methanol in methylene chloride. Fractions were combined based upon TLC. ^{1}H NMR resonances indicative of DSP related compounds were not detected.

The *P. maculosum* hexane extract (*Pm*HH) was dried, suspended in methanol (1 ml), applied to an LH-20 column (2 x 23.5 cm) and eluted with two column volumes of methanol. Fractions were combined based on TLC. *Pm*HH2 contained compounds visualized on TLC with heat as baseline, mid-plate and upper plate pink staining spots. *Pm*HH2 was dried onto silica packing, applied to a silica column (1 x 13 cm) and eluted with a methylene chloride in methanol gradient identical to that described for *Pm*HM2. Fractions were combined based on TLC.

*Pm*HH3 from the initial LH-20 column separating the hexane extract was dried onto silica, applied to a silica column (2 x 40 cm) and eluted successively with four column volumes of methylene chloride-ethyl acetate-methanol (100 : 0 : 0, 95 : 5 : 1, 90 : 10 : 1, and 70 : 30 : 2). Fractions were combined based on TLC and ^{1}H NMR data were collected. Resonances indicative of DSP related compounds were absent.

*Pm*HH3-9 gave a non-polar spot on TLC, which turned bright fuscia with vanillin 2 upon heating (R_f = 0.81; 7.5 : 4 : 1 toluene-acetone-methanol). This sample was tested for ichthyotoxicity. Symptoms of toxicity were observed beginning at 0.5 h, with

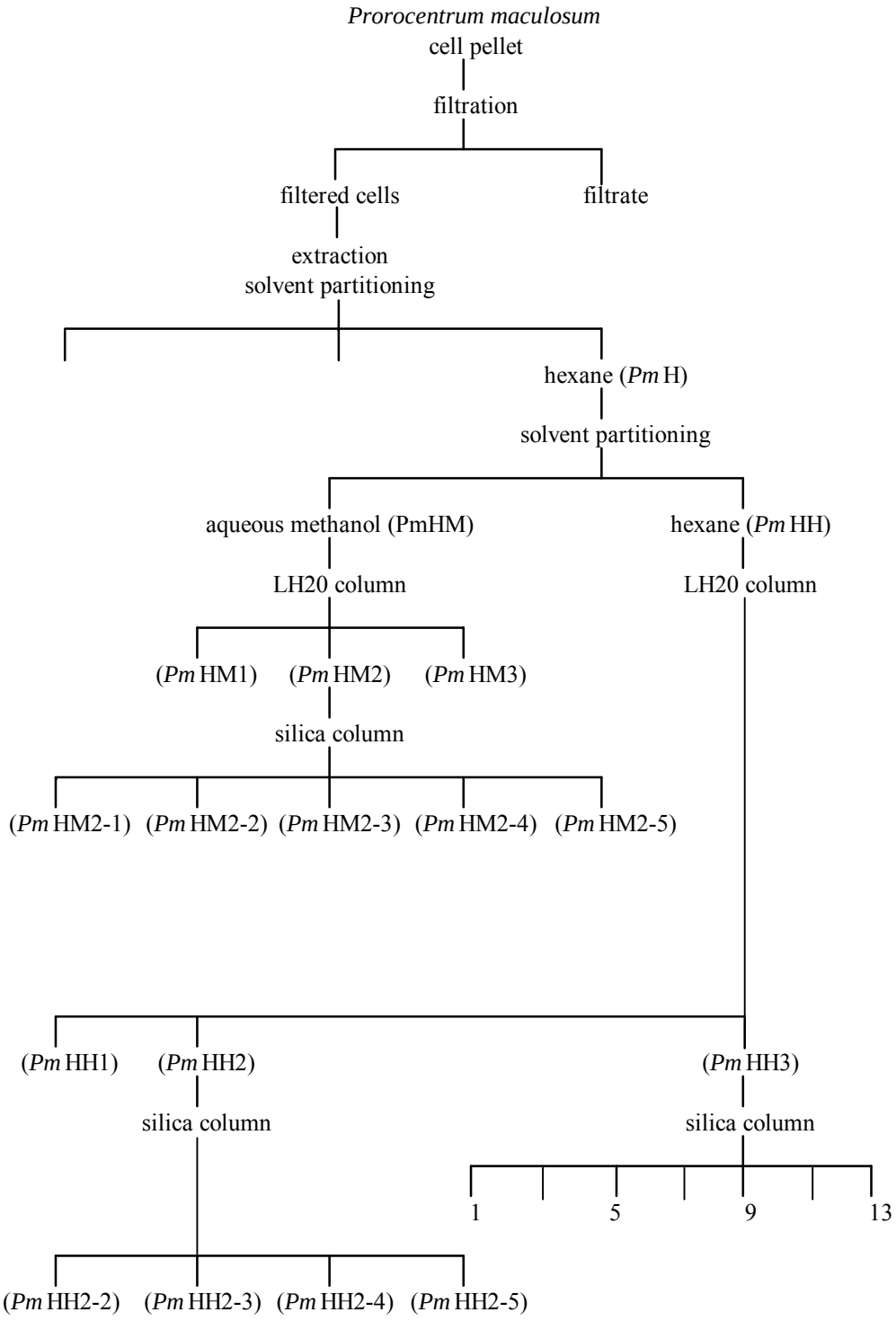

Figure 8. *Pm*H fractionation scheme.

duration a minimum of 8 h. 24 h after the commencement of the experiment, the experimental fish was again comparable in behavior with the control.

A portion of *Pm*HH3-9 (5 mg) was subsequently methylated by refluxing with methanol / BF_3 (1 ml) for 30 minutes at 80 °C and extracted with hexane (1 ml x 3). The hexane extract was applied to a silica column and eluted with 40 % ether in hexane. The material eluted from the silica column was analyzed by GC/MS. ^{1}H NMR data are reported below.

*Pm*HH3-9 (80.1 mg): ^{1}H NMR (400 MHz) in $CDCl_3$ δ 5.33 (10H, m), 2.80 (8H, m), 2.34 (5H, m), 2.06 (5H, m), 1.55 (4H, m), 1.27 (1H, p), 1.22 (24 H, m), 0.93 (3H, t, J = 7.25 Hz), 0.84 (3H, t, J = 6.99 Hz).

1D and 2D NMR experiments were performed on *Pm*HH3-1, containing a single neon pink staining TLC spot. An aliquot of *Pm*HH3-1 was dissolved in acetonitrile and injected onto an analytical Vydac C_{18} column (4.6 x 250 mm; elution 99% acetonitrile; flow rate 1 ml/min; UV monitoring).

Upon analysis by TLC, a non-polar compound isolated from *P. maculosum* (*Pm*HH3-1) quenched UV light and stained neon pink (vanillin 2; R_f = 0.23; 100 % methylene chloride). ^{1}H and ^{13}C NMR data for *Pm*HH3-1 are reported below.

*Pm*HH3-1 (1.2 mg): UV λ max (acetonitrile) 205nm; ^{1}H NMR (400 MHz) in $CDCl_3$ δ 5.37 (1H, t, J = 6.93 Hz), 4.11 (2H, d, J = 6.17 Hz), 1.95 (2H, t, J = 7.80 Hz), 1.63 (3H, s), 1.50 (1H, sept, J = 6.64 Hz), 1.35-1.44 (4H, m), 1.03-1.30 (14H, m), 0.82 (6H, d, J = 6.80 Hz), 0.80 (3H, d, J = 6.73 Hz), 0.78 (3H, d, J = 6.54 Hz); ^{13}C NMR (400 MHz) in $CDCl_3$ δ 123.0, 59.4, 39.9, 39.3, 37.4, 37.3, 37.3, 36.6, 32.8, 32.7, 28.0, 25.1, 24.8, 24.4, 22.7, 22.6, 19.7, 19.7, 16.2.

The ethyl ether extract from the initial partitioning of *P. maculosum* cells (*Pm*E) was dried, suspended in methanol (0.5 ml), applied to a LH-20 column (1.2 x 25.5 cm) and eluted with two column volumes of methanol. The fractionation scheme for the *P. maculosum* ethyl ether extract is shown in Figure 9. Fractions were combined based on TLC and tested for antibacterial, antifungal and ichthyotoxic activity. The combination of fractions exhibiting antibacterial activity (*Pm*E3) was dried onto Bakerbond C_{18} packing, applied to a Bakerbond C_{18} column (1 x 10 cm) and eluted with 5 to 95 % methanol. Fractions exhibiting antibacterial activity (*Pm*E3-1) were again combined and subjected to TLC. TLC analysis of the antibiotic mixture *Pm*E3-1 revealed two TLC spots (R_f = 0.50 and R_f = 0.55; 7.5 : 4 : 1 toluene-acetone-methanol) which stained yellow (vanillin 2) and pink (vanillin 1), upon heating. The mixture was separated on a Zorbax C_{18} column (9.4 x 250 mm; elution gradient 20 to 80 % methanol; flow rate 2.5 ml/min; 30 min.). Two compounds (*Pm*E3-1-1 and *Pm*E3-1-2) were separated and examined by TLC analysis and antibacterial testing. ^{1}H and ^{13}C NMR were performed on *Pm*E3-1-1. Biological and analytical data for *Pm*E3-1-1 and *Pm*E3-1-2 are reported below.

*Pm*E3-1-1 (4.5 mg): inhibition (*P. aeruginosa*) 4906 AU, (*B. subtilis*) 3315 AU, (*E. coli*) 3925 AU; ^{1}H NMR (400 MHz) in CD_3OD δ 5.34 (1H, q, J = 5.50 Hz), 1.30 (3H, d, J = 5.50 Hz) ^{13}C NMR (400MHz) in CD_3OD δ 105.4, 18.4.

*Pm*E3-1-2 (0.7 mg): inhibition (*P. aeruginosa*) 7707 AU, (*B. subtilis*) 5240 AU, (*E. coli*) 6231 AU.

The filtrate obtained from the *P. maculosum* cells prior to cell extraction was dried, resuspended in methanol (50 ml) and filtered to remove a large portion of salt from

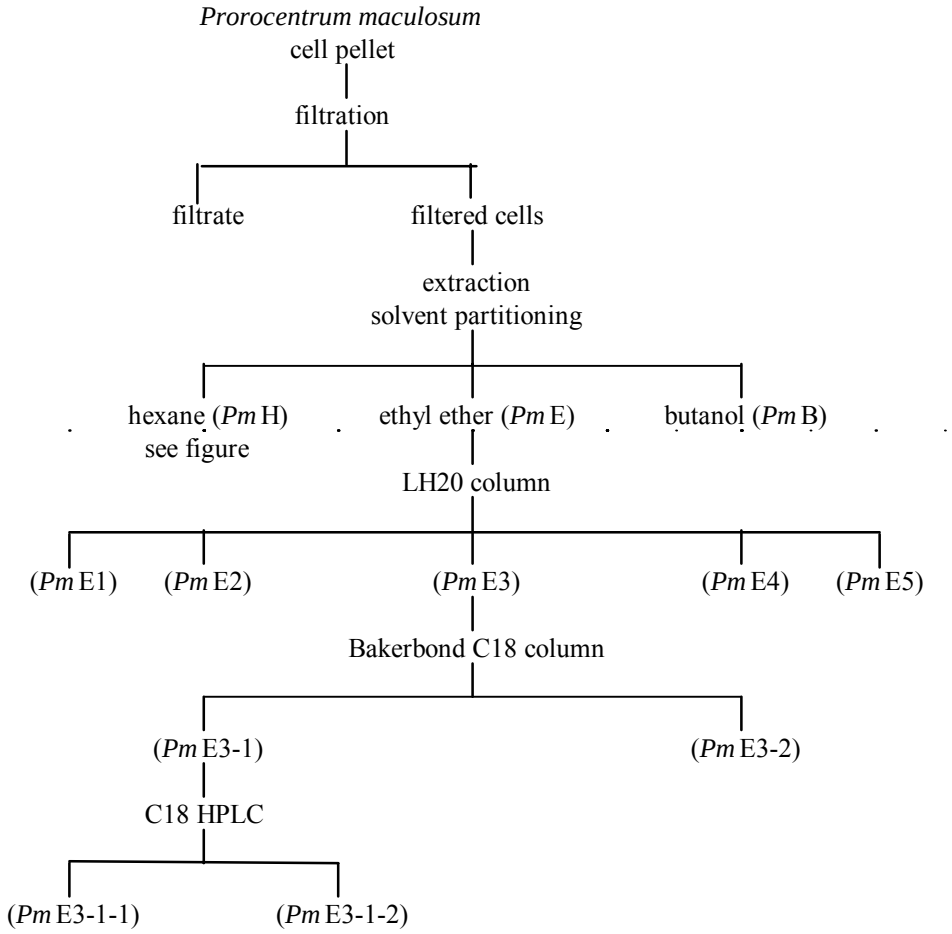

Figure 9. *Pm*E fractionation scheme.

the mixture. The fractionation scheme for the filtrate from the *P. maculosum* cells is shown in Figure 10. The filtrate was dried, resuspended in methanol (0.5 ml), applied to an LH-20 column (1.5 x 22 cm) and eluted with two column volumes of methanol. Fractions were combined based on analysis by TLC. Fractions containing a TLC spot corresponding to an okadaic acid standard (*Pm*F2—stained pink upon spraying and turned mauve upon heating) were combined and applied to a silica column (1 x 21 cm), and eluted with methanol-methylene chloride (5, 10, 20, 40, 60, and 100%). Fractions were combined based on TLC. Fractions containing a TLC spot matching the okadaic acid standard were combined and dried. Chloroform (1 ml) was added to the dried material (*Pm*F2-2), gently swirled and removed to separate fatty contaminants from the mixture. The remaining material containing okadaic acid (*Pm*F2-2-M) was suspended in methanol (0.5 ml), applied to an LH20 column (1 x 23 cm), and eluted with two column volumes of methanol. Two main fractions, *Pm*F2-2-M1 and *Pm*F2-2-M2, were analyzed by TLC and ^{1}H NMR. *Pm*F2-2-M1 appeared identical to an okadaic acid standard in TLC analysis (stained pink with vanillin 2 upon spraying; R_f = 0.25; 7.5 : 4 : 1 toluene-acetone-methanol). The ^{1}H NMR spectrum (CD_3OD) matched that of an authentic sample of okadaic acid obtained from Crain. Additional analytical data for *Pm*F4-4-M1 follows.

*Pm*F2-2-M1 (0.8 mg): UV λ max (acetonitrile / 0.1 % TFA) 205 nm; esims $[MNa]^+$ 827.5; $[MNa - 18]^+$ 809.5; $[MNa – 18 - 18]^+$ 791.5; $[MNa – 560.4]^+$ 267.1.

P. lima

P. lima cells (9 L) were harvested by centrifugation in Sept., 2002, and the cell pellet placed in a boiling water bath (15 min) to denature the esterase and lipase enzymes.

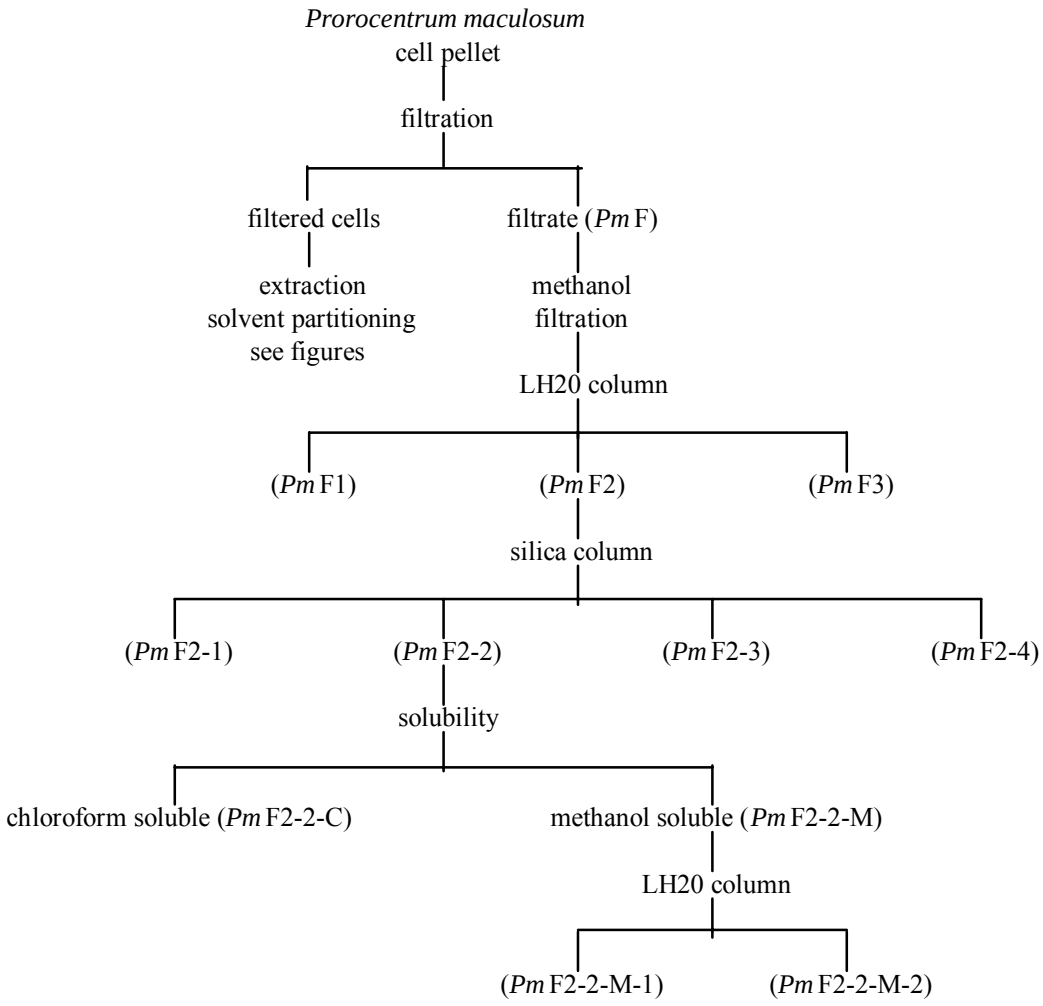

Figure 10. *Pm*F fractionation scheme.

The cell filtrate was added to the aqueous methanol extract of the cells prior to partitioning. Extraction and partitioning were performed as described previously and is shown in Figure 11. The hexane extract (*Pl*H) was dried, resuspended in 50% methanol (50 ml) and shaken against hexane (4 x 50 ml). The aqueous methanol extract (*Pl*HM) was dried, resuspended in methanol, applied to an LH-20 column (1 x 15.5 cm) and eluted with two column volumes of methanol. Fractions were combined based on TLC.

The *P. lima* ethyl ether extract fractionation scheme is shown in Figure 12. The ethyl ether extract of the *P. lima* cells (*Pl*E) was dried, resuspended in 25% methanol (50 ml) and shaken against ethyl ether (2 x 50 ml). The aqueous methanol extract (*Pl*EM) was dried, resuspended in methanol (0.5 ml), applied to an LH-20 column (1 x 15.5 cm) and eluted with two column volumes of methanol. Fractions were combined based on TLC. ^{1}H NMR was performed on *Pl*EM1, *Pl*EM2, and *Pl*EM3. Resonances indicative of DSP related compounds were absent in the ^{1}H NMR spectra of *Pl*EM1 and *Pl*EM3. *Pl*EM2 contained both a TLC spot matching the okadaic acid standard and ^{1}H NMR resonances indicative of DSP related compounds.

*Pl*EE was dried, resuspended in methanol (0.5 ml), applied to an LH20 column (1 x 15.5 cm) and eluted with two column volumes of methanol. Fractions were combined based upon TLC. ^{1}H NMR was performed on *Pl*EE1, *Pl*EE2, and *Pl*EE3. TLC and NMR analysis of *Pl*EE1 and *Pl*EE3 indicated the absence of DSP related compounds. *Pl*EE2 contained ^{1}H NMR resonances indicative of DSP related compounds in addition to a TLC spot that matched the okadaic acid standard.

TLC analysis of the antibiotic mixture *Pl*EE4 revealed two TLC spots (R_f = 0.50 and R_f = 0.55; 7.5 : 4 : 1 toluene-acetone-methanol) which stained yellow (vanillin 2) and

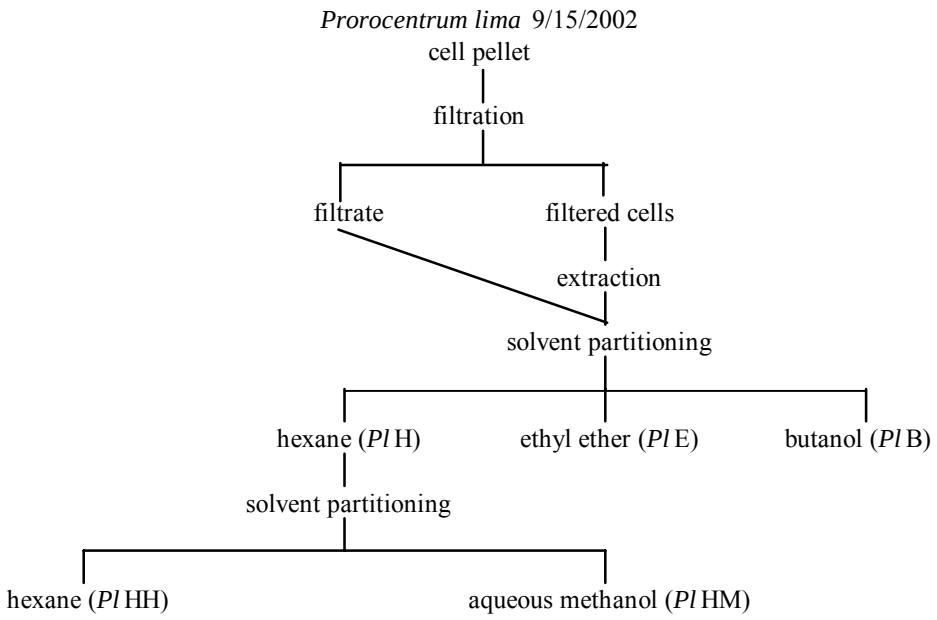

Figure 11. *Pl*H fractionation scheme.

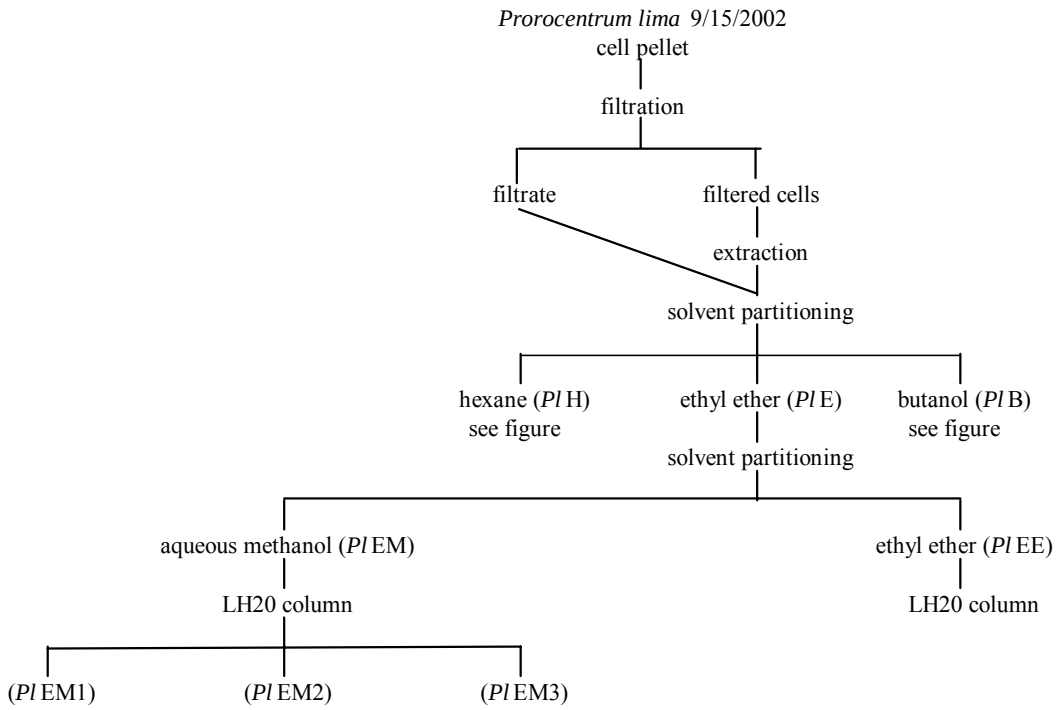

Figure 12. *Pl*E fractionation scheme.

pink (vanillin 1), upon heating. *Pl*EE4 was dried, suspended in 20 % methanol and purified by the same HPLC method as *Pm*E3-1. Isolated peaks *Pl*EE4-1 and *Pl*EE4-2 were tested for antibacterial activity. ^{1}H and ^{13}C NMR were performed on *Pl*EE4-1. Biological and analytical data for *Pl*EE4-1 is reported below.

*Pl*EE4-1 (1.3 mg): inhibition (*P. aeruginosa*) 4538 AU, (*B. subtilis*) 3243 AU, (*E. coli*) 3750 AU; ^{1}H NMR (400 MHz) in CD_3OD δ 5.34 (1H, q, J = 5.50 Hz), 1.30 (3H, d, J = 5.50 Hz) ^{13}C NMR (400MHz) in CD_3OD δ 105.4, 18.4.

*Pl*EE4-2 (.2 mg): inhibition (*P. aeruginosa*) 7425 AU, (*B. subtilis*) 5890 AU, (*E. coli*) 6020 AU.

The *P. lima* butanol extract was fractionated as shown in Figure 13. The butanol extract (*Pl*B) was dried, resuspended in methanol and filtered to remove excess salt. The filtrate (*Pl*BM) was dried, resuspended in methanol (1 ml), applied to an LH-20 column (2 x 33 cm), and eluted with two column volumes of methanol. Fractions were combined based on TLC and ^{1}H NMR was performed. Resonances indicative of DSP related compounds were not detected.

DMSO (1 ml) was added to dried *Pl*BM1, swirled and removed. The remainder of the mixture was dissolved in methanol (1 ml). ^{1}H NMR was recorded for *Pl*BM1D. *Pl*BM4 was dried onto silica packing, applied to a silica column (1 x 15 cm) and eluted with methanol-methylene chloride (30, 40, 50, 60, and 100 %). Fractions were combined based on TLC and ^{1}H NMR data obtained for *Pl*BM4-1 and *Pl*BM4-2. *Pl*BM4-1 was dried, suspended in methanol (0.5 ml), applied to an LH-20 column (1 x 10 cm) and eluted with two column volumes of methanol. Fractions were combined based on TLC.

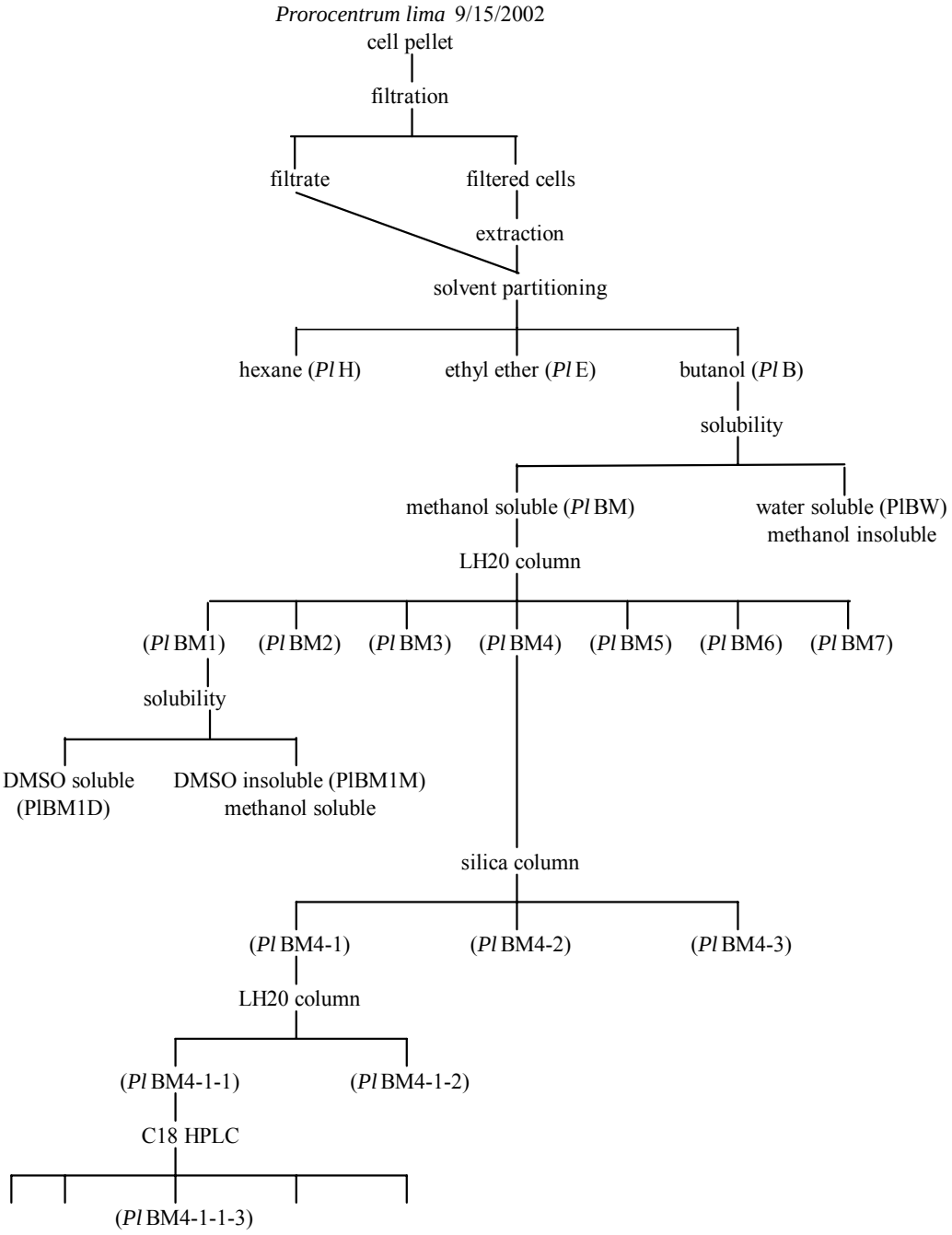

Figure 13. *Pl*B fractionation scheme.

*Pl*BM4-1-1 contained a mid-plate pink spot upon heating a TLC plate (mobile phase ethyl acetate-isopropanol-water; 8 : 3 : 1). Preparative HPLC of PlBM4-1-1 was performed on a Vydac C_{18} column (4.6 x 250 mm; 20 – 80 % acetonitrile; 1 ml/min; 20 min). ^{1}H NMR data were recorded for *Pl*BM4-1-1-3, the pink staining TLC spot. Resonances indicative of DSP related compounds were absent.

A second culture of *P. lima* cells (12 L) was harvested by centrifugation in Jan., 2003 and the centrifuge tubes immediately placed in a boiling water bath (15 min). Extraction and partitioning were performed as described previously. The ethyl ether extract (*Pl*2E) contained a TLC spot that, like the okadaic acid standard, stained pink upon spraying but demonstrated a higher R_f value (Rf = 0.45; 7.5 : 4 : 1 toluene-acetone-methanol; vanillin 2). The fractionation scheme for this *P. lima* ethyl ether extract is shown in Figure 14. *Pl*2E was dried, resuspended in methanol (1 ml), applied to an LH-20 column (2 x 36 cm) and eluted with two column volumes of methanol, and fractions combined based upon TLC. The combination of fractions containing the spot that stained pink upon spraying (*Pl*2E2) was applied to a silica column (1 x 26.5 cm) and eluted with methanol-methylene chloride (5, 10, 20, 30, 40, 50 and 60 %). Fractions were combined based upon TLC. The combination of fractions containing the spot that stained pink upon spraying (*Pl*2E2-2) was dried and subjected to ^{1}H and COSY NMR. LC/MS was performed using a Zorbax C_{18} column (2 x 50 mm; elution gradient 40 to 70 % acetonitrile / 0.1 % TFA; flow rate 0.4 ml/min). *Pl*2E2-2 was tested for activity in the cell-signaling assay (see Table 2). The ^{1}H NMR spectrum of *Pl*2E2-2 matched that of an authentic sample of okadaic acid with the exception of the following detectable resonances.

Sample Name	Mass (ug)	B-galactosidase Activity (Miller Units)	
		Sample	Control
Pm E3-1-1	30	314	405
Pl E2-2	30	352	405
Pl S1-1-2	30	395	405
Pl S1-1-4	30	362	405
Pl EA	50	296	276
	150	409	313
Pl EA1	100	379	336
Pl EA2	100	345	336
Pl EA3	100	363	336
Pl EA4	100	561	336
Pl EA5	100	390	336
Pl EA6	100	347	336
Pl 2EA	100	442	336
Pl 2EA4	100	429	315
Pl EA4-1	8	333	313
Pl EA4-2	19	329	313
Pl EA4-3	21	336	313
Pl EA4-4	40	298	313
Pl EA4-5	57	350	313
Pl EA4-6	12	295	313

Table 2. Cell-signaling assay results for *Prorocentrum* metabolites.

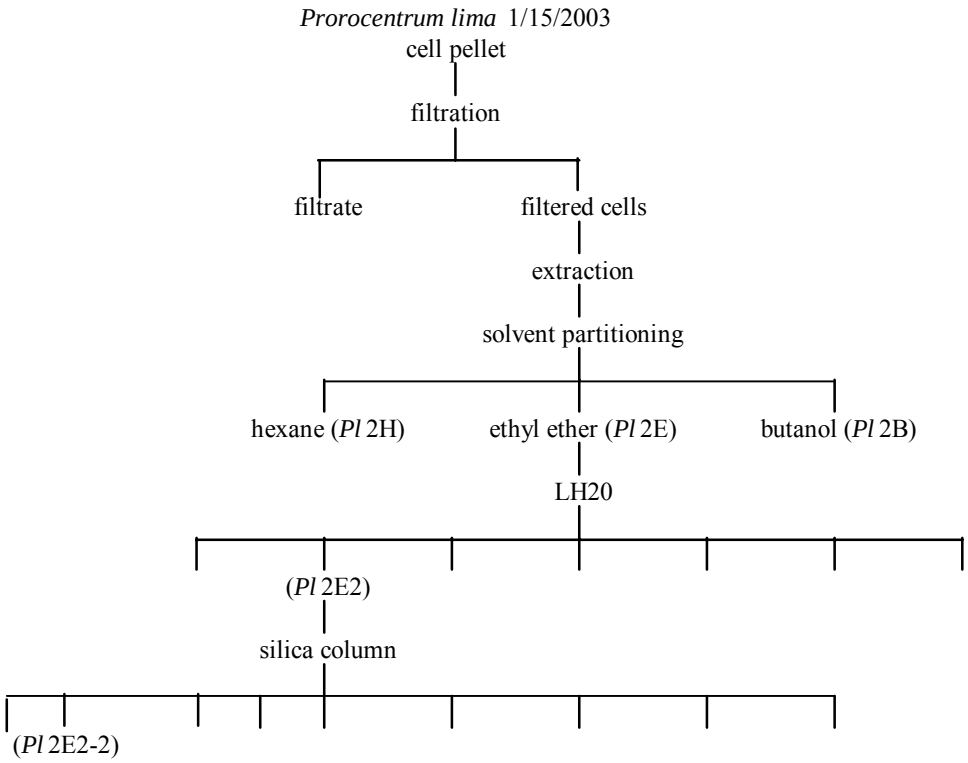

Figure 14. *Pl*2E fractionation scheme.

*Pl*2E2-2 (mixture of *Pl*2E2-2a-d): ^{1}H NMR (400 MHz) in $CDCl_3$ additional resonances δ 6.30, 6.05, 5.92, 5.70, 5.49, 4.87, 4.74, 4.65, 3.64, 2.61, .2.37, 1.69, 0.85.

Analytical data for the components of *Pl*2E2-2 follows. *Pl*2E2-2a: UV λ max (acetonitrile) 238 nm; esims $[MNa]^+$ 951.5, $[MNa-124]^+$ 827.5. *Pl*2E2-2b: UV λ max (acetonitrile) 234 nm; esims $[MNa]^+$ 965.6, $[MNa-138]^+$ 827.5. *Pl*2E2-2c: UV λ max (acetonitrile) 238 nm; esims $[MNa]^+$ 977.5, $[MNa-150]^+$ 827.5 *Pl*2E2-2d: UV λ max (acetonitrile) 238 nm; esims $[MNa]^+$ 965.5, $[MNa-124]^+$ 841.5

The fractionation scheme for the corresponding butanol extract is shown in Figure 15. The butanol extract (*Pl*2B) was dried, suspended in methanol (1 ml), applied to an LH-20 column (2 x 36 cm), and eluted with two column volumes of methanol. Fractions were combined based on TLC. The combination of fractions was applied to a C_{18} Sep Pack column (6 ml) and eluted with aqueous methanol (5 to 95 %). Fractions were combined based on TLC and ^{1}H NMR was performed on fraction *Pl*2B1-7. Pl2B1-7 contained a single fuscia staining TLC spot (Rf = 0.05; 7.5 : 4 : 1 toluene-acetone-methanol; vanillin 2). The ^{1}H NMR spectrum was very similar to that of *Pm*HH3-9 with additional resonances between 3.5 and 4.5 ppm.

The fractionation scheme for the *P. lima* cell free culture media is shown in Figure 16. The supernatant remaining after ultracentrifugation was applied to a conditioned C_{18} Sep Pak (60 ml) previously washed with DI water. The column was eluted with aqueous methanol (20, 40, 60, 80 and 100 %). Fractions were analyzed by TLC and compared with an okadaic acid standard. Fractions containing spots matching the okadaic acid standard were combined, dried, resuspended in methanol and applied to an LH-20 column (1x 15 cm). The column was eluted with two column volumes of

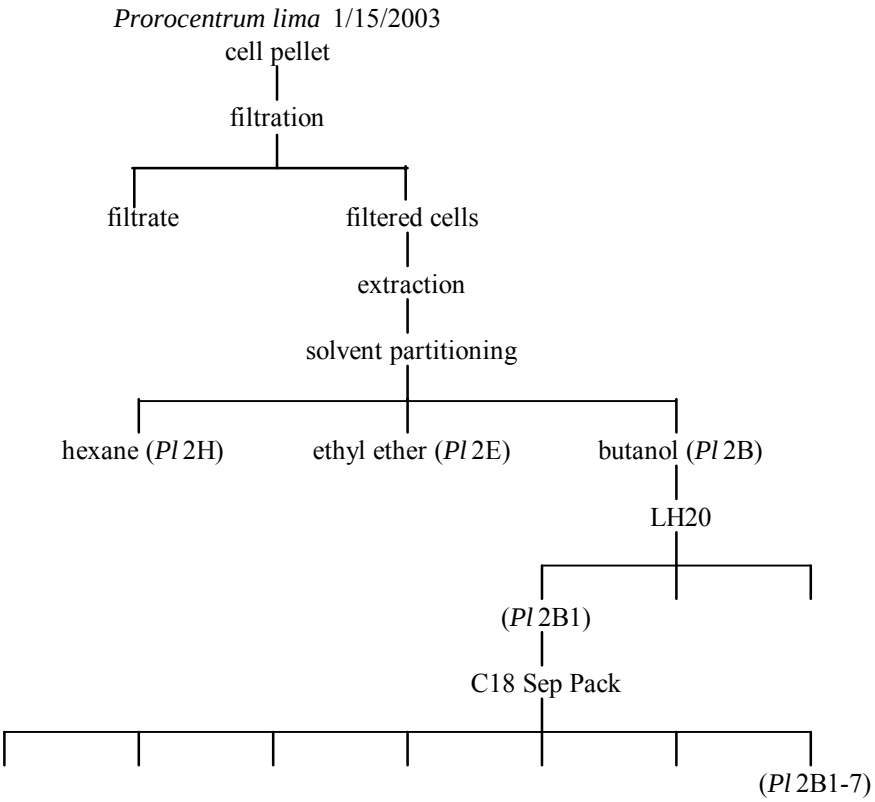

Figure 15. *Pl*2B fractionation scheme.

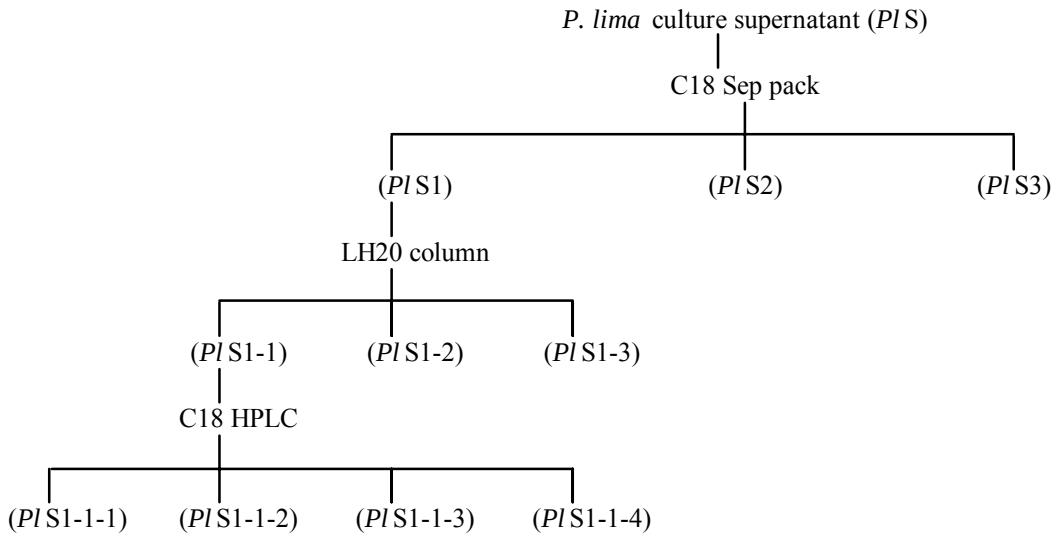

Figure 16. *Pl*S fractionation scheme.

methanol and fractions collected. Fractions containing spots matching the okadaic acid standard were combined, dried and subjected to LC/MS. The sample was separated by a Zorbax C_{18} column (2 x 50 mm; elution 60 % acetonitrile / 0.1 % TFA; flow rate .21 ml/min; see Figure 17).

The mixture was separated by preparative HPLC using a Lumina C_{18} column (4.6 x 250 mm; elution 65 % acetonitrile / 0.1 % TFA; flow rate 1ml/min). Three individual compounds, *Pl*S1-1-2, *Pl*S1-1-3 and *Pl*S1-1-4, were collected and subjected to the cell-signaling bioassay (see Table 2) and ^{1}H NMR. Analytical data on the three individual components of *Pl*S1-1 are reported below.

*Pl*S1-1-2 (0.7 mg): UV λ max (acetonitrile / 0.1 % TFA) 205 nm; esims $[MNa]^+$ 827.5; $[MNa - 18]^+$ 809.5; $[MNa – 18 - 18]^+$ 791.5; $[MNa – 560.4]^+$ 267.1 (R_t = 2.1 min.; Zorbax C18; 2 x 50 mm; 60 % acetonitrile / 0.1 % TFA; 0.21 ml/min). The ^{1}H NMR spectrum of PlS1-1-2 ($CDCl_3$) was identical to that of an authentic sample of okadaic acid.

*Pl*S1-1-3 (0.1 mg): UV λ max (acetonitrile / 0.1 % TFA) 205 nm; esims $[MNa]^+$ 841.5; $[MNa - 18]^+$ 823.5; $[MNa – 18 - 18]^+$ 805.5; $[MNa – 560.4]^+$ 267.1 (R_t = 3.0 min.; Zorbax C18; 2 x 50 mm; 60 % acetonitrile / 0.1 % TFA; 0.21 ml/min). ^{1}H NMR spectrum ($CDCl_3$) matched that of an authentic sample of okadaic acid, with the exception of one additional detectable resonance (δ 0.88) and the shift of the ^{1}H resonance on C-30 from 3.26 to 3.29 ppm.

*Pl*S1-1-4 (1.2 mg): UV λ max (acetonitrile / 0.1 % TFA) 205 nm; esims $[MNa]^+$ 841.5; $[MNa - 18]^+$ 823.5; $[MNa – 18 - 18]^+$ 805.5; $[MNa – 560.4]^+$ 267.1 (R_t = 4.3 min.; Zorbax C18; 2 x 50 mm; 60 % acetonitrile / 0.1 % TFA; 0.21 ml/min). The ^{1}H NMR

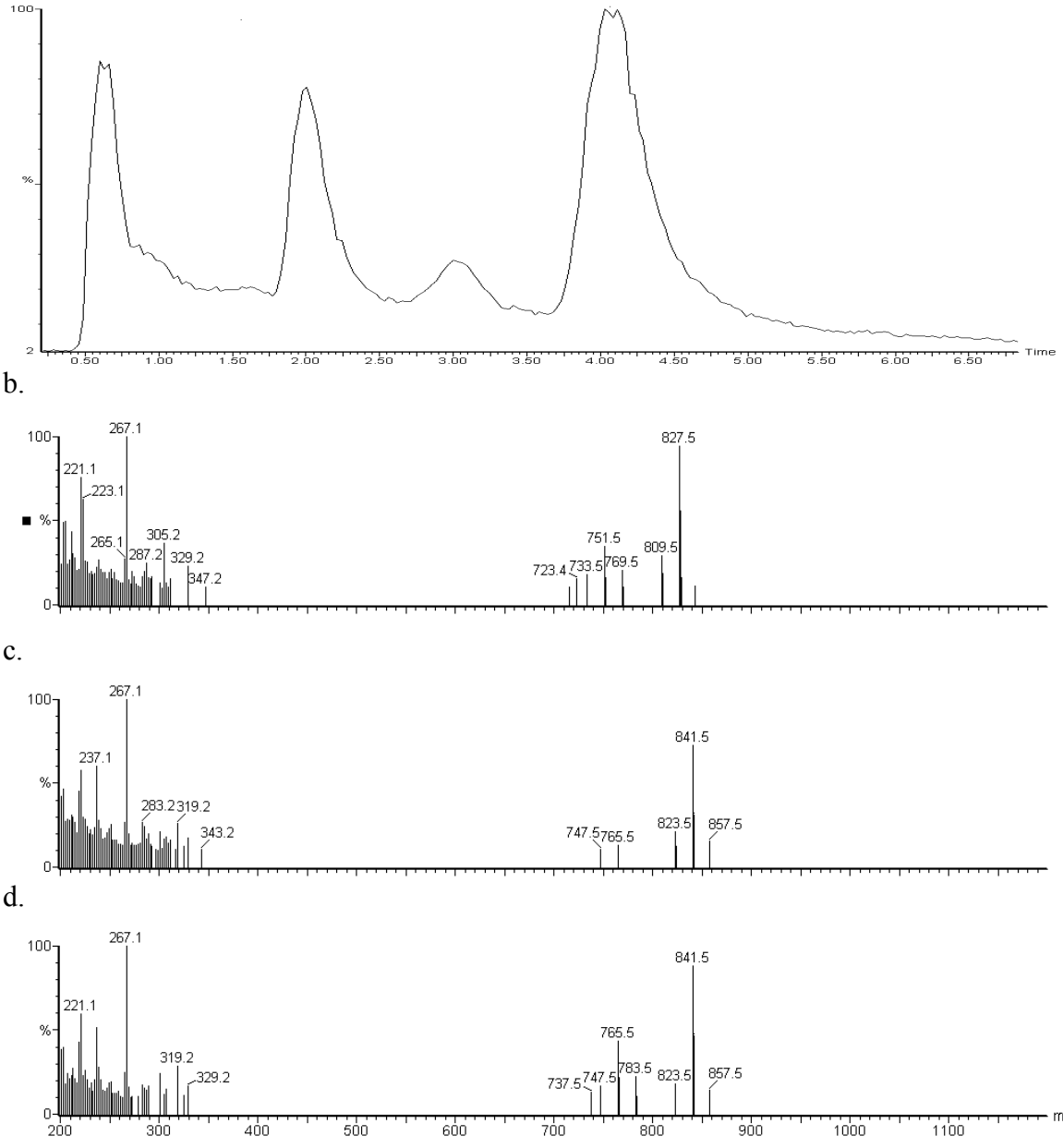

Figure 17. LC/MS data for *P. lima* DSP free acid isolates.
- a.) *Pl*S1-1 chromatogram.
- b.) *Pl*S1-1-2 mass spectrum.
- c.) *Pl*S1-1-3 mass spectrum.
- d.) *Pl*S1-1-4 mass spectrum.

spectrum ($CDCl_3$) matched that of an authentic sample of okadaic acid, with the exception of one additional detectable resonance (δ 0.90).

P. lima culture (8 L) was carefully decanted on May 5, 2003 and the reduced volume containing the cells centrifuged (2000 rpm; 4 °C; 5 min). The supernatant was carefully removed and the cells placed in a boiling water bath (15 min). Cell extraction was performed as previously described and TLC analysis was performed on all the extracts.

The decanted culture media from the *P. lima* cells was filtered and the filtrate partitioned against ethyl acetate (2 L). The fractionation scheme is shown in Figure 18. The ethyl acetate extract (*Pl*EA; 10.2 mg) was dried, resuspended in acetonitrile (20 ml) and filtered. The filtrate was dried, resuspended in 50 % acetonitrile / 0.1 % TFA, and applied to a Vydac C_{18} column (4.6 x 250 cm; elution gradient 40 to 90 % acetonitrile / 0.1 % TFA; flow rate 0.4 ml/min; 60 min). MS data was collected. An aliquot of the extract was tested for cell signaling activity (see Table 2).

Preparative HPLC was performed on the ethyl acetate extract using a Vydac C_{18} column (9.4 x 250 mm; elution gradient 50 to 99 % methanol; flow rate 2 ml/min; 30 min). Six fractions (*Pl*EA1-*Pl*EA6) were collected and tested for activity in the cell-signaling assay (see Table 2). 1D and 2D NMR were performed on the mixture *Pl*EA4 (400μg). Resonances indicative of DSP related compounds were detected by ^1H NMR. *Pl*EA4 was fractionated on a Vydac C18 column (4.6 x 250mm; 70-99% methanol in 3mM formic acid; 30 min.; 1 ml/min.). Half of each of the six fractions (PlEA4-1 through PlEA4-6) was tested in the cell signaling bioassay (see Table 2).

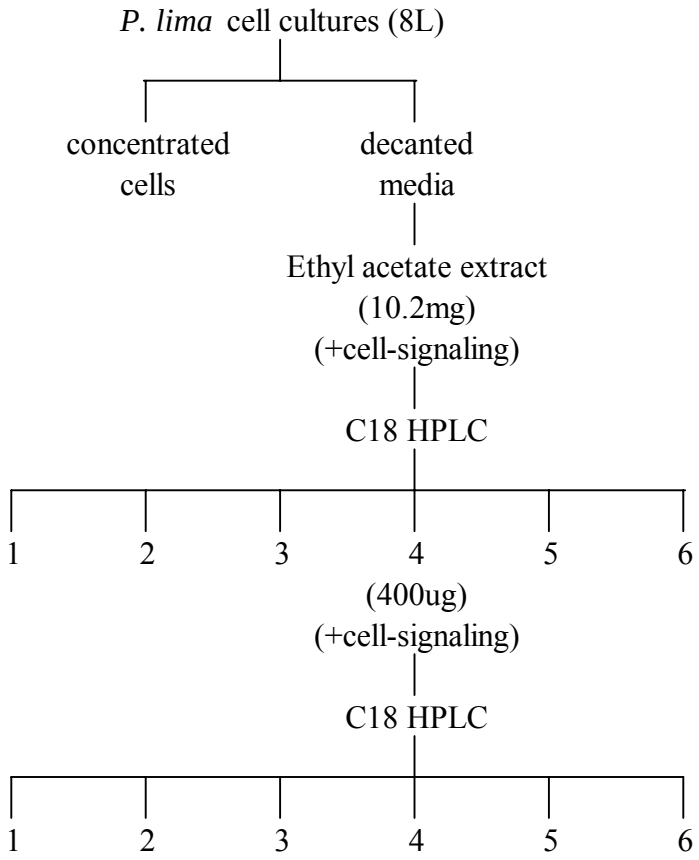

Figure 18. Fractionation of active *P. lima* cell-signaling mixture.

Another batch of *P. lima* cells (8 L) was carefully decanted on May 15, 2003 and the reduced volume containing the cells centrifuged (2000 rpm; 4 °C; 5 min). The supernatant was decanted and the cells were placed in a boiling water bath (15 min) as before. Cell extraction was performed as previously described and TLC analysis was performed on the extracts.

The decanted culture media from the *P. lima* cells harvested in May 15, 2003 was filtered and the filtrate partitioned against ethyl acetate (2 L). The ethyl acetate extract (*Pl*2EA; 6.4 mg) was dried, resuspended in acetonitrile (20 ml) and filtered. A portion of the extract was tested for cell signaling activity (see Table 2). Preparative HPLC was performed on the remainder of the extract using a Vydac C_{18} column (9.4 x 250 mm; elution gradient 50 to 99 % methanol; flow rate 2 ml/min: 30 min). The fraction (*Pl*2EA4) matching the chromatogram of the earlier active fraction (*Pl*EA4) was collected and tested for activity in the cell-signaling assay.

Efficient Isolation Method for DSP Toxins

An additional batch of *P. lima* cells (42 L) was harvested in July, 2003. The filtered, decanted culture media was extracted with ethyl acetate (10 L) and analyzed by LC/MS. $[MNa]^+$ equal to 828.5 and 841.5 were detected in the mixture.

The remaining cells, concentrated in culture media (1 L), were frozen, thawed and sonicated (x 2) to induce release of DSP toxins to the media. The fractionation scheme developed for efficient isolation of the toxins is shown in Figure 19. The cell debris was filtered and the filtrate concentrated on 6 individual C_{18} Sep Pack columns (60 ml; elution 20, 40, 60, 80 and 100% aqueous methanol). Fractions were analyzed by TLC and LC/MS. A TLC spot matching the okadaic acid standard was detected in the 60 %

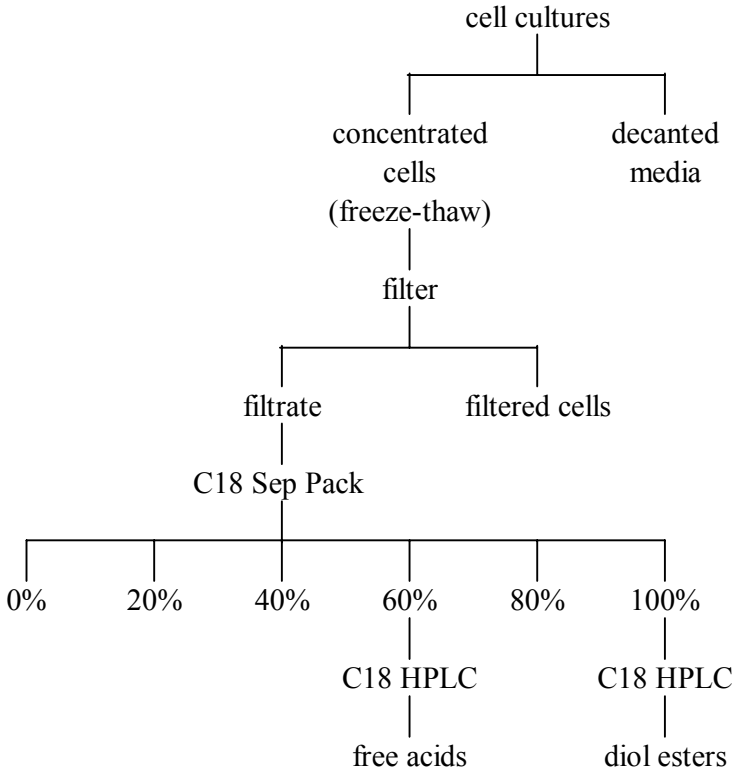

Figure 19. Efficient isolation method for DSP compounds.

methanol fractions. LC/MS of the 60% methanol fraction (Zorbax C_{18}; 2 x 50mm; elution 60 % acetonitrile / 0.1 % TFA, flow rate 0.21 ml/min) revealed several peaks including OA, DTX-1 and a peak that eluted between the two demonstrating a mass fragmentation pattern identical to that of DTX-1. Purification of these three compounds by preparatory HPLC was accomplished using a Luna C_{18} column (4.6 x 250mm, 60% acetonitrile / 0.1 % TFA, 1 ml/min).

A more non-polar TLC spot matching *Pl*2E2-2 (Rf = 0.45; 7.5 : 4 : 1 toluene-acetone-methanol; vanillin 2) was detected in the 100% methanol fractions eluted from the C_{18} Sep Pack columns. LC/MS was performed using a Zorbax C_{18} column (2 x 50 mm; elution gradient 40 to 70 % acetonitrile / 0.1 % TFA; flow rate 0.4 ml/min). Several compounds present in the mixture generated molecular ions identical to the compounds in *Pl*2E2-2. Each compound contained a mass fragment equal to either 827.5 or 841.5, the masses of OA and DTX-1 respectively. One compound contained a molecular ion (m/z) equal to 841.5.

The filtered cell debris was extracted with aqueous methanol (80 %; 500 ml x 2), and the extract analyzed by TLC. A non-polar bright fuscia TLC spot was detected (R_f = 0. 0.80; 7.5 : 4 : 1 toluene-acetone-methanol) in addition to a polar fuscia TLC spot (Rf = 0.05; 7.5 : 4 : 1 toluene-acetone-methanol; vanillin 2).

LC/MS of Cell-Signaling Compounds

An LC/MS method was developed to detect five known cell-signaling compounds. N-butyryl-DL-homoserine lactone (C_4HSL), N-hexanoyl-DL-homoserine lactone (C_6HSL), and N-dodecanyl-DL-homoserine lactone (C_{12}HSL) were purchased from Sigma-Aldrich, 3-oxo-dodecanoyl homoserine lactone (3-oxo-C_{12}HSL) was

purchased from Quorum Biosciences, Inc., and PQS was donated by the Pesci lab. Each compound (100 μg) was suspended in 50 % acetonitrile / 0.1 % TFA (800 μl). Aliquots (20 μl) of this mixture were injected onto a Vydac C_{18} column (4.6 x 250 cm; elution gradient 40 to 90% acetonitrile / 0.1 % TFA in 30 min.; flow rate 0.4 ml/min). The chromatogram generated from LC/MS of five known cell signaling molecules is shown in Figure 20. Data is reported below.

C_4HSL: retention time 7.5 min.; esims $[MH]^+$ 172; $[MH - 70]^+$ 101.9.

C_6HSL: retention time 9.5 min.; esims $[MH]^+$ 200; $[MH - 98]^+$ 101.9.

PQS: retention time 16.8 min.; esims $[MH]^+$ 260; $[MH - 85]^+$ 175.

$3OC_{12}$HSL: retention time 21.5 min.; esims $[MH]^+$ 298; $[MH - 196]^+$ 101.9.

C_{12}HSL: retention time 27.2 min.; esims $[MH]^+$ 284; $[MH - 182]^+$ 101.9.

Pa2P4-2-2-10, PlEA4, and Pl2EA4 were each analyzed by the LC/MS method developed for the detection of known signaling compounds. The five known cell-signaling molecules analyzed were not detected in these active samples. These samples were also scanned by LC/MS for all possible molecular ions that could be formed from the two known *P. aeruginosa* cell-signaling diketopiperazines. Cyclo(ΔAla-L-Val) and cyclo (L-Pro-L-Tyr) were not detected in the samples.

Two compounds with molecular ions of 841.7 and exhibiting different retention times were detected during the LC/MS analysis of *Pl*EA4. MS spectra for these two compounds are shown in Figure 21.

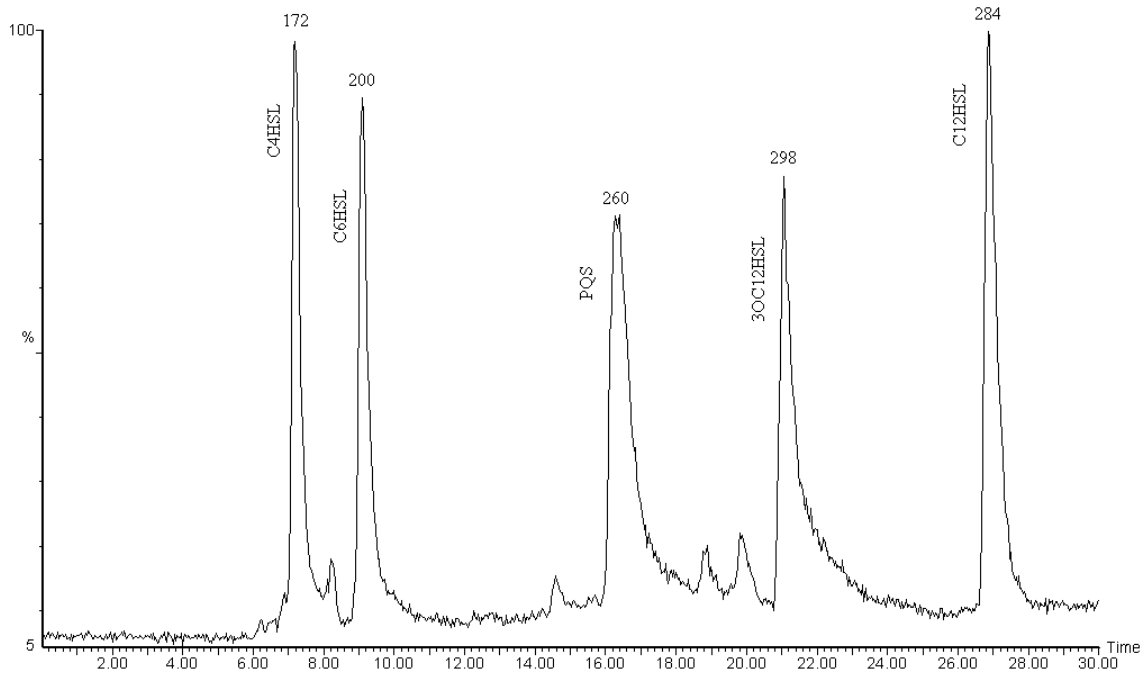

Figure 20. LC/MS of cell signaling compounds.

a.

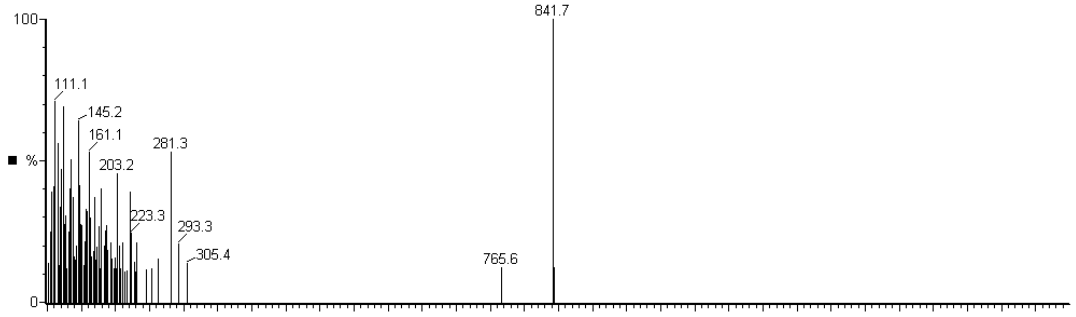

b.

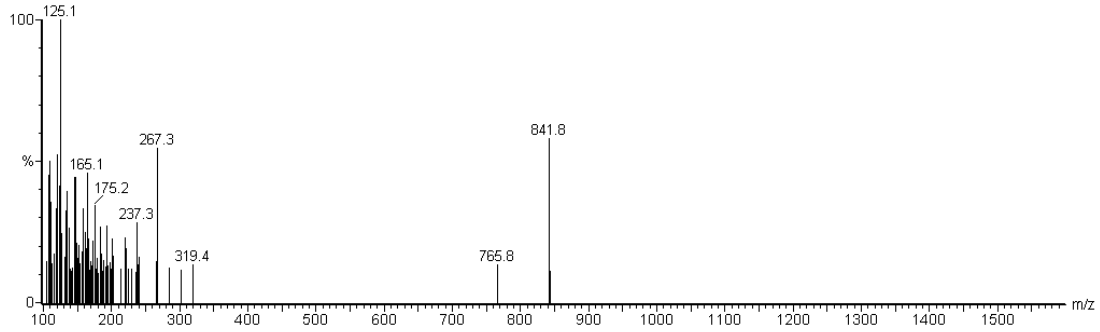

Figure 21. Mass spectra of DTX-1 and a new methyl derivative of OA.
a.) *Pl*EA4a (DTX-1 isomer).
b.) *Pl*EA4b (DTX-1).

RESULTS

Characterization of *P. aeruginosa* Antibiotic Isolates

Fractionation of *Pa*2P, the precipitate from *P. aeruginosa* culture supernatant (8 L), yielded sufficient material for purification and biochemical characterization of five known antibiotic metabolites (Pa2P4-2-2-5, 6, 9, 10, and 11). Demonstrating activity against *B. subtilis,* the five related compounds were eluted isocratically from the C_{18} column in order of increasing molecular weight $[MH]^+$ (244 - 288). Each antibiotic generated two UV maxima in 45 % acetonitrile / 0.1 % TFA, an intense band in the range 230 - 260 nm and a less intense band in the range 300 - 320 nm.

COSY and HMQC data for 4-hydroxy-2-nonylquinoline (1), the structure proposed for *Pa*2P4-2-2-10, are shown in Figure 22. MS and UV data were consistent with the structure of this known *P. aeruginosa* metabolite: $[MH]^+$ 272, and the major fragment ion $[MH - C_8H_{17}]^+$ equal to 159 ($[C_{10}H_8NO]^+$) (Royt et al., 2001). ^{13}C NMR results indicated nine aliphatic carbons, consistent with an alkyl chain, and six aromatic carbons. Three quaternary aromatic carbons could not be observed due to the limited amount of sample available (< 1 mg). The DEPT spectrum revealed eight CH_2 groups, with chemical shifts ranging from 33.6 – 22.3 ppm. The aromatic carbon resonance at 133.2 ppm was not present in the DEPT spectrum or the HMQC, indicating a quaternary carbon. Compound (1) is a mixture of keto-enol tautomers (see Figure 23), reported to exist primarily as the 4-hydroxy-2-alkylquinoline (Royt et al., 2001).

Based upon the structure of (1) and analytical data from the related compounds isolated concurrently, the structures of *Pa*2P4-2-2-5, 6, 9, and 11 were identified. While *Pa*2P4-2-2-5 (2) and (1) both contained the same major fragment ion (*m/z* 159), the

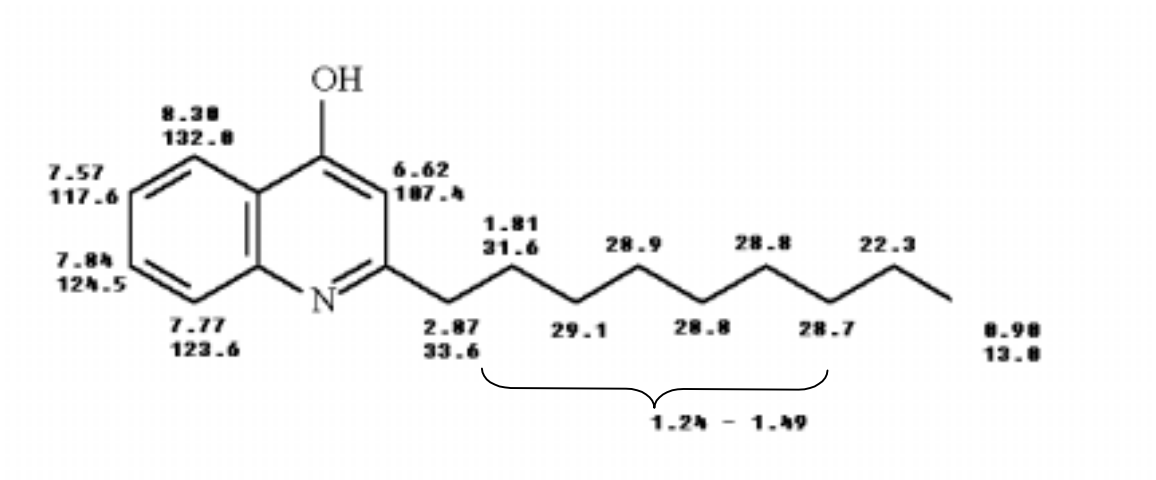

^{1}H chemical shift (ppm)	Coupling	Coupled ^{1}H chemical shift (ppm)
8.30	d	7.57
7.84	t	7.77, 7.57
7.77	d	7.84
7.57	t	8.30, 7.84
6.62	s	N/A
2.87	t	1.81
1.81	p	2.87, 1.24 – 1.49
1.24 – 1.49	m	1.81, 0.90
0.90	t	1.24 – 1.49

Figure 22. 4-hydroxy-2-nonylquinoline structural assignments. ^{1}H and ^{13}C chemical shifts (ppm) are shown on the structure. COSY data for each proton resonance are shown in the table.

a.

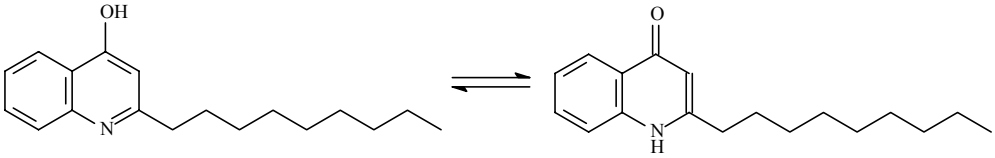

b.

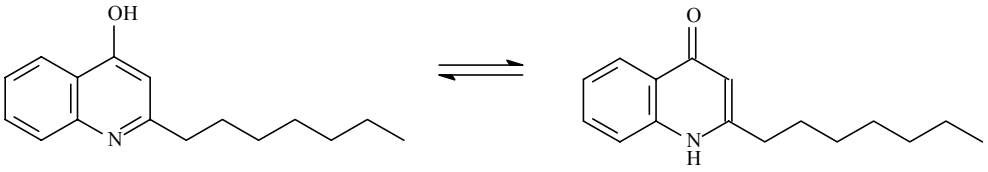

c.

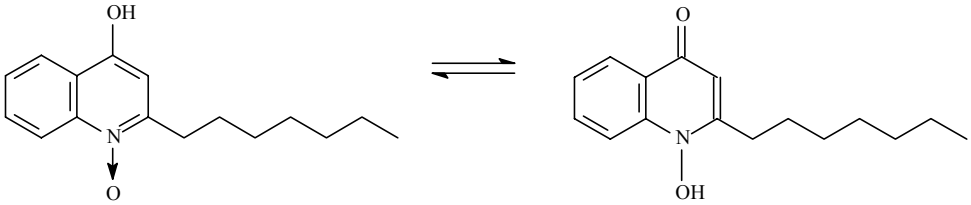

d.

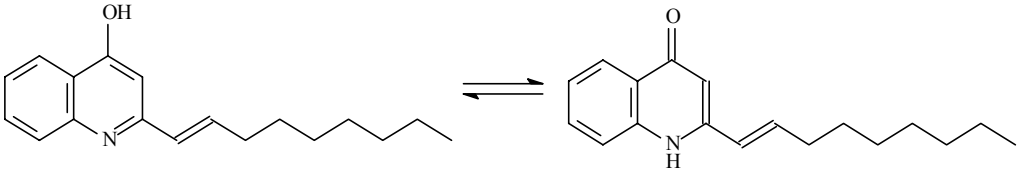

e.

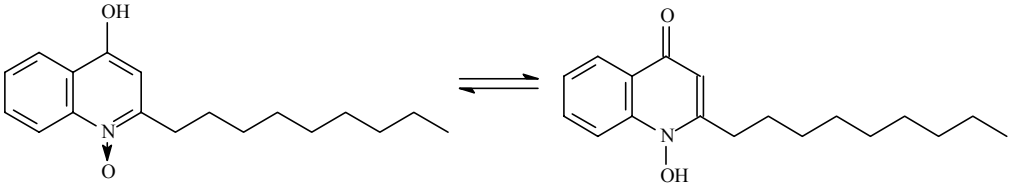

Figure 23. 4-hydroxy-2-alkyl/alkenyl quinolines.
- a.) 4-hydroxy-2-nonylquinoline (1)
- b.) 4-hydroxy-2-heptylquinoline (2)
- c.) 4-hydroxy-2-heptylquinoline-N-oxide (3)
- d.) 4-hydroxy-2-nonenylquinoline (4)
- e.) 4-hydroxy-2-nonylquinoline-N-oxide (5)

$[MH]^+$ of the molecular ion for (2) was 28 amu lower suggesting a loss of two CH_2 groups from the alkyl chain. Compound (2) was therefore identified as 4-hydroxy-2-heptylquinoline (Figure 23b). The ^1H NMR of (2) was nearly identical to that of (1), but lacked four aliphatic protons, yielding additional evidence in support of structure (2).

The $[MH]^+$ ion of *Pa*2P4-2-2-6 (3) was 16 amu higher than (2) and this compound was identified as 4-hydroxy-2-heptylquinoline-N-oxide (Figure 23c). LC/MS data for (3) showed a loss of 16 amu, consistent with the loss of oxygen from an N-oxide, and the same major fragment ion (*m/z* 159) as seen in both (1) and (2), indicating a hydroxyquinoline structure. The ^1H NMR spectrum of (3) was similar to that of the ^1H NMR spectrum of (2), with the exception of a major chemical shift change for one aromatic proton. The doublet at δ 7.77 ppm in the spectrum of (2) and assigned to H-8, appeared at δ 8.17 ppm in (3), due to the deshielding effect of the N-oxide function (see Figure 22).

*Pa*2P4-2-2-9 (4) was identified as 4-hydroxy-2-nonenylquinoline (Figure 23d). The $[MH]^+$ ion for (4) is 2 amu less than (1), suggesting the presence of an additional degree of saturation. The ^1H NMR spectrum of (4) was consistent with this, and contained resonances for two additional olefinic protons, coupled with the absence of four aliphatic protons. Several pieces of data were used to locate the portion of the double bond with the alkyl chain. First, the increase in UV absorbance compared with (1) indicates an additional degree of conjugation, which would only occur if the double bond were in conjugation with the aromatic system. Secondly, one of the new olefinic proton resonances in (4) was a clean doublet (J = 16 Hz) demonstrating trans coupling with no other coupling, while the second olefinic resonance appeared as a doublet of

triplets. This coupling pattern can only be satisfied by placement of the double bond in the side chain as shown.

*Pa*2P4-2-2-11 (5) was identified as 4-hydroxy-2-nonylquinoline-N-oxide (Figure 23e). The $[MH]^+$ of (5) equaled that of (1) plus 16 amu, indicating that (5) is the N-oxide of (1). MS data for (5) showed a molecular ion $[MH]^+$ equal to 288 and the loss of 16 amu in the creation of a fragment ion, consistent with the loss of oxygen. Like the other compounds in the series, (5) contained the same major fragment ion (159) seen in (1), (2), (3) and (4), consistent with a hydroxyquinoline structure. The ^1H NMR spectrum of (5) was also similar to that of (1), with the exception of a major chemical shift change for one olefinic proton. The doublet at δ 7.77 in the spectrum of (1) assigned to H-8 now appeared at δ 8.16 in (5), to generate an aromatic region identical to that of 4-hydroxy-2-heptylquinoline-N-oxide (3).

Fractionation of the organic extract of the *P. aeruginosa* culture supernatant on LH-20 yielded an antibiotic mixture (*Pa*E2-2), identical in TLC analysis to *Pa*1P4-4-2. Analytical work performed on the mixture using HPLC/UV, LC/MS and NMR revealed two major components of *Pa*E2-2. Compound *Pa*E2-2-3 (6) was active against all bacterial strains tested, with the exception of the parent strain of *P. aeruginosa*. The spectroscopic data for the major components of PaE2-2-3 (6) was consistent with the known *P. aeruginosa* antibiotic pyoluteorin (Figure 2c). Particularly characteristic was the 9 : 6 : 1 ratio of the three $[MH]^+$ ions spaced by two daltons, indicative of the presence of two chlorine atoms in the molecule, due to the 3 : 1 isotope ratio of ^{35}Cl to ^{37}Cl. The resonance at δ 185.7 ppm in the ^{13}C NMR spectrum suggested the presence of a carbonyl, while the remaining resonances were consistent for aromatic and olefinic

carbons, with several shifted downfield due to bonding with electron-withdrawing groups. COSY data indicated that the protons with δ 7.08 ppm (1H) and 6.37 ppm (2H) were attached to adjacent carbons.

The UV spectrum of the second compound, *Pa*E2-2-4 (7) displayed an intense peak at 248nm and a smaller one at 368 nm, characteristic of a phenazine. Only signals in the aromatic region of the ^{1}H NMR spectrum were observed, consistent with a phenazine-1-carboxamide or phenazine-1-carboxylic acid structure. The $[MH]^{+}$ (*m/z* 224) of (7) corresponds to phenazine-1-carboxamide (Figure 24), a known inhibitor of plant root fungal pathogens (Jayatilake et al., 1996). Interestingly, in this work, no inhibition was detected against the bacterial or fungal assay strains tested.

Metabolites of *Prorocentrum* species

P. maculosum Ichthyotoxic Isolates

A non-polar isolate from the *P. maculosum* hexane extract (*Pm*HH3-9) demonstrated ichthyotoxicity against *G. toxicus*, causing the fish to invert and convulse for hours. The TLC and ^{1}H NMR data for *Pm*HH3-9 indicate a mixture of saturated and unsaturated free fatty acids, which was confirmed by GC/MS analysis. In the ^{1}H NMR data, the 10 : 8 : 3 ratio for resonances at 5.33 ppm : 2.80 ppm : 0.93 ppm suggested the presence of structure (8), octadecapentaneoic acid [18:5(n-3)] (Figure 25) (Kuklev et al., 1992). This toxic polyunsaturated fatty acid is commonly found in dinoflagellates, and comprised approximately 50 % of the mixture by ^{1}H NMR analysis. The fatty acid (8) is thought to be synthesized within the chloroplast and exist as a component of the

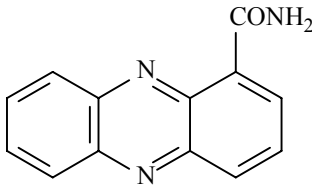

Figure 24. Phenazine-1-carboxamide (7)

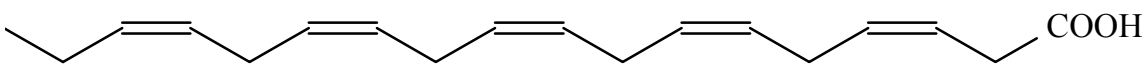

Figure 25. Octadecapentaenoic acid (8)

glycolipid thylakoid membrane (LeBlond and Chapman, 2000), and are released as free fatty acids from the glycolipid upon hydrolysis of the ester bond.

. Interestingly, no fish toxicity was detected in an organic extract of boiled *P. lima* cells. In addition, no free fatty acids were detected by TLC or NMR analysis. However, a large quantity of more polar compounds that stained the same color as the free fatty acids (vanillin spray # 2) were detected. ^{1}H NMR of these fractions revealed a fatty acid signature similar to that seen in (8), with additional carbohydrate resonances consistent with a possible glycolipid structure for *Pl*2B1-7 in the mixture (Hauksson et al., 1995).

The apparent inverse relationship between free fatty acids and glycolipids in cell extracts would support the hypothesis that the free fatty acids in *P. maculosum* were initially components of glycolipids. Hydrolysis of the ester bond would release free fatty acids from glycolipids. It is interesting to note that the parent molecules of okadaic acid are also believed to be synthesized within the chloroplasts of the dinoflagellate cell (de Traubenberg et al., 1995) and that the okadaic acid is released as a result of enzyme hydrolysis. It is possible that the esterases responsible for releasing free fatty acids are also responsible for the hydrolysis releasing DSP free acids from the sulfated diesters. The abundance of free fatty acids in the unboiled *P. maculosum* cells and their absence in the boiled *P. lima* cells supports this hypothesis. An additional extraction was performed on unboiled *P. lima* cells to test this hypothesis. As expected, TLC spots matching the compounds previously identified as fatty acids and glycolipids were both detected in analysis of the cell extract. However, additional NMR and MS analysis of the purified compounds is necessary to confirm their identity.

Additional Metabolites from *Prorocentrum* Species

The ^{1}H NMR spectrum for *Pm*HH3-1 (9) is identical to that published for phytol, a chlorophyll breakdown product (Hayamizu et al., 2003). Phytol (Figure 26) was isolated incidentally from the *P. maculosum* cell extract during the search for non-polar okadaic acid diol esters. Phytol, the ester-linked side chain of chlorophyll-a, is released from the macromolecule through hydrolysis of the ester bond. Ubiquitous in the marine environment, phytol is commonly used as a phytoplankton biomarker (Rontani and Volkman, 2003).

Characterization of OA, DTX-1 and Two New Methyl Derivatives of OA

Previously identified DSP toxins produced by *Prorocentrum* species include OA, DTX-1 (35-methyl OA), and DTX-2 (Figure 27). During this study, OA, DTX-1 and two new methyl derivatives of OA were isolated.

The ^{1}H NMR spectrum of *Pm*F2-2-M1 (10), isolated from the *P. maculosum* cell-free culture media, was identical to that of OA. In addition, the molecular ion of (10) when analyzed by electrospray ionization mass spectrometry (positive ion mode) appeared at *m/z* 827.5, corresponding to the sodium adduct of OA, commonly formed when using this analytical technique. The fragmentation pattern of (10) was also consistent with published data for okadaic acid, exhibiting a series of fragments with losses of 18 amu (H_2O) in addition to a major fragment at *m/z* 267. This key fragment ion appears in the ESI-MS of all known DSP toxins and corresponds to the molecular component $C_{14}H_{21}O_6$ minus 18 amu (H_2O) (Figure 27) (Sakai and Rinehart, 1995).

LC/MS analysis showed that the *P. lima* culture supernatant concentrated on the C_{18} Sep Pack contained three DSP toxins, OA, DTX-1, and a new methyl derivative of

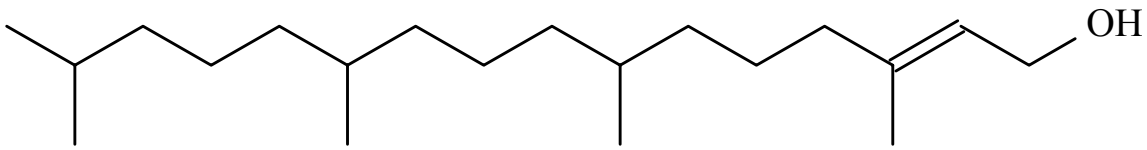

Figure 26. Phytol (9)

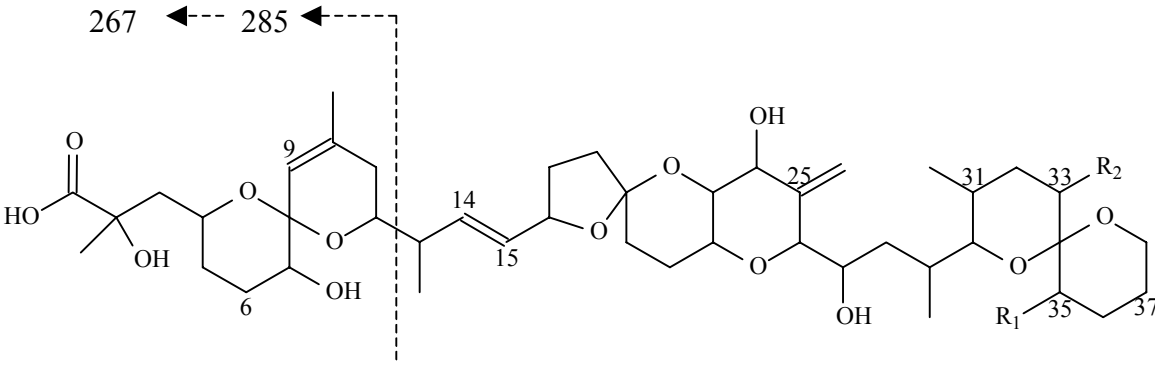

Compound	R_1	R_2
OA (10)	H	H
DTX-1 (11)	CH_3	H
33-methyl OA (12)	H	CH_3

Figure 27. Mass fractionation of OA, DTX-1, and 33-methyl OA.

OA. Analytical data generated for *Pl*S1-1-2 (10), isolated from the *P. lima* cell-free supernatant, was identical to that reported for OA. LC/MS and NMR data for a second major component, *Pl*S1-1-4 (11), were consistent with DTX-1, which contains an additional methyl group at C-35 (Yasumoto et al., 1985).

A minor component *Pl*S1-1-3 (12) displayed the same molecular weight ($[MH]^+$ 841.5) as DTX-1 by LC/MS analysis. The MS data for this minor component was helpful in locating the position of the methyl group. The characteristic fragment ion at *m/z* 267 observed in the ESI-MS spectrum of OA and DTX-1, was also observed in this methyl okadaic acid isomer, indicating that the methyl is located on the right hand side of the molecule (see Figure 27). Key resonances in the main skeleton of the compound were unchanged ($CDCl_3$) (δ 5.66, 5.48, 5.44, 5.32, 5.06, 4.56, 1.04, 1.02, 0.90), indicating that the carbon skeleton of new compound was very similar to that of OA. The proton signal for the new methyl group in (12) appeared at higher field (δ_H 0.88 ppm) than the signal for the additional methyl group in DTX-1 (δ_H 0.90 ppm). Based on the biosynthesis of DSP toxins (Wright et al., 1996; MacPherson et al., 2003), additional methyl goups are possible at C-17, C-21, C-33 and C-37. The new location of the methyl group was determined by inspection of the adjacent CH-O protons at C-16 (C-17 methyl substitution), C-22 (C-21 methyl substitution, C-30 (C-33 substitution), and C-38 (C-37 substitution). No discernable differences were detected in the ^1H NMR resonances generated by protons on C-16, C-22 and C-38 between (11) and (12). However, in the NMR spectrum of (12) the proton resonance for C-30 demonstrated a slight downfield chemical shift (δ_H 3.29 ppm) compared with the proton resonance for C-30 in DTX-1 (δ_H 3.26 ppm). The coupling pattern of the C-30 proton resonance remained unchanged,

signifying the presence of the methyl on C-31. The change in chemical shift is hypothesized to be a result of the presence of a methyl on C-33, the only other possible location for methyl substitution on the ring containing C-30, and hence (12) is tentatively characterized as 33-methyl OA (Figure 27).

An extract partially purified from the cell-free decanted culture media contained both DTX-1 (*Pl*EA4b) and a second methyl OA derivative. This methyl OA derivative gave a different mass fragmentation pattern than either OA, DTX-1, or 33-methyl OA, in that it showed a major fragment ion of 281 instead of 267. This indicated that the extra methyl group is located on the left hand side of the molecule (C1-C13) (see Figure 27). The methyl ester of OA could account for this phenomenon, which has been observed before as an artifact of the extraction process using methanol (Holmes et al., 1999). However, this new methyl derivative was present in crude extracts monitored by LC/MS prior to exposure of the sample to methanol. Furthermore, the methyl ester of OA is very non-polar and would not elute from a HPLC column between OA and DTX-1. Several options are possible for the placement of this additional methyl group: it could be part of a methyl ether moiety at C-2 or C-7, or it could be directly attached to the carbon backbone. If the latter case were true, then the biosynthetic results (Wright et al., 1996; MacPherson et al., 2003) would predict that C-6 is the only plausible position for this new methyl group.

Characterization of *P. lima* Diol Esters

The diol esters are a naturally occurring group of esters of OA and DTX-1. The ^{1}H NMR spectra of the mixture was similar to those of OA or DTX-1, but contained

additional resonances associated with the ester function. The seven largest additional resonances detected in the diol mixture (δ 6.30, 6.05, 5.70, 4.65, 3.64, 2.37, 1.69) were present. Six of these resonances (δ 6.30, 6.05, 5.70, 4.65, 3.64, 2.37) demonstrated coupling in the COSY experiment. The major resonances could be readily assigned to the resonances for a previously reported diol (Figure 28) (Hu et al., 1993).

Analytical data supported the identification of *Pl*2E2-2a (13) as a C_8 diol ester of OA (Figure 29). The parent ion appeared at $[MNa]^+$ *m/z* 951.5 and showed a major fragment ion at m/z 827.5 consistent with the Na adduct of OA. The alcohol moiety ($C_8H_{13}O$) contained two degrees of unsaturation and the UV max (acetonitrile / 0.1% TFA) at 238 nm indicated the presence of two conjugated double bonds.

A second ester, *Pl*2E2-2d (14), was identified as the C_8 diol ester of DTX-1. The molecular ion of the diol ester (14) ($[MH]^+$ *m/z* 965.5) indicated the presence of an additional methyl group, while a key fragment ion at *m/z* 841.5 corresponded to the Na adduct of DTX-1. The molecular weight of this compound as well as the UV maximum (λ max = 238 nm) is consistent with the diol structure shown in Figure 28 attached to DTX-1 (Figure 29) (Hu et al., 1993).

Of the remaining mixture, trace amounts of an OA C_9 diol ester, *Pl*2E2-2b (15) were detected by LC/MS, but further structural determination of the diol moiety was not possible due to the lack of material. OA C_9 diol esters with three alternate side chain structures have been described in the literature, each containing two double bonds (Hu et al., 1992). In this case, the UV data for the OA C_9 diol ester (15) was similar to that of (13) and (14), indicating the presence of a conjugated diene system in the diol moiety. Only one C_9 diol ester has been described containing a conjugated diene system and a

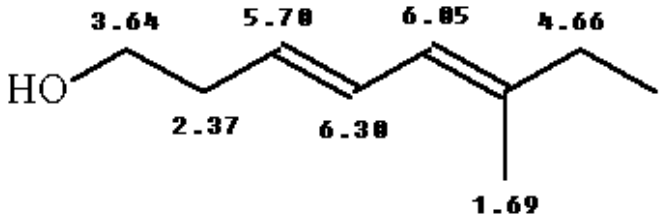

^{1}H chemical shift (ppm)	Coupled ^{1}H chemical shift (ppm)
6.30	6.05, 5.70, 2.37
6.05	6.30, 5.70, 4.65
5.70	6.30, 6.05, 2.37
4.65	6.05
3.64	2.37
2.37	3.64, 5.70, 6.05, 6.30
1.69	N/A

Figure 28. Proposed diol side chain.

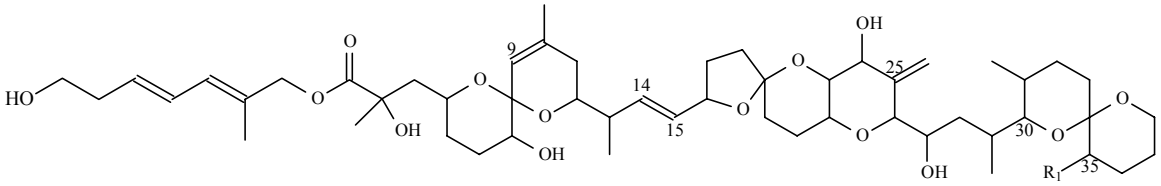

Compound	R_1
OA C_8 diol ester (13)	H
DTX-1 C_8 diol ester (14)	CH_3

Figure 29. *P. lima* OA C_8 diol and DTX-1 C_8 diol isolates.

tentative structure is proposed (Figure 30a). Definitive identification requires additional material necessary for further NMR experiments.

Yet another diol was observed in trace amounts and the LC/MS data indicated it was a C_{10} diol ester of OA. The molecular weight (m/z 977.5) of this ester was 12 amu more than the OA C9 ester, indicating the addition of one carbon and no hydrogens, and therefore an additional degree of saturation. The UV data (λ_{max} 238 nm) revealed that only two of the double bonds are in conjugation and a tentative structure for (16) is shown in Figure 30b. More material is required to complete the structural analysis.

Cell-signaling Activity

P. aeruginosa Isolates

Pyoluteorin and the phenazines have been shown to be regulated by quorum sensing compounds(Stead et al., 1996; Bloemberg and Lugtenberg, 2001), although no known *P. aeruginosa* autoinducers were detected in the LC/MS analysis of culture extracts in this study. Autoinducer activity was, however, detected by bioassay in a simple mixture isolated from the *P. aeruginosa* culture extracts (*Pa*2P4-2-2-10). Purification of (1), the major component of this mixture, resulted in decreasing activity at each stage of purification. ^{1}H NMR spectra of the purified fractions *Pa*2P4-2-2-10, *Pa*2P4-2-2-10-2, and *Pa*2P4-2-2-10-2-1 are shown in Figure 31. Several of the "contaminant" components of the active mixture were also tested for activity, but exhibited no induction or only slight induction of the assay strain.

a.)

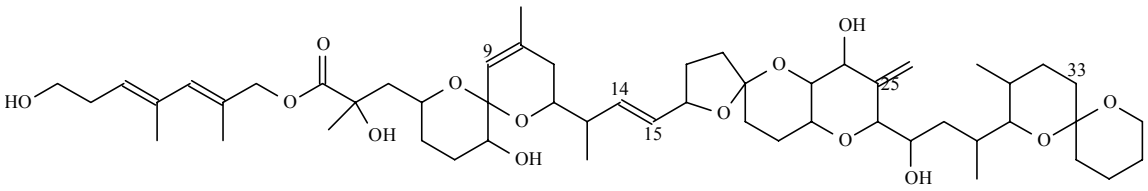

b.)

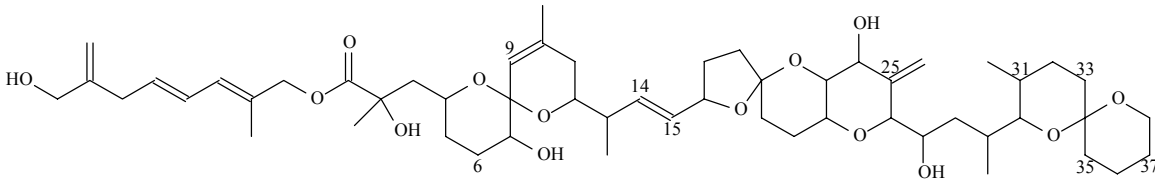

Figure 30. Tentative structures for OA C_9 diol ester and OA C_{10} diol ester.
a.) OA C_9 diol ester (15).
b.) OA C_{10} diol ester (16).

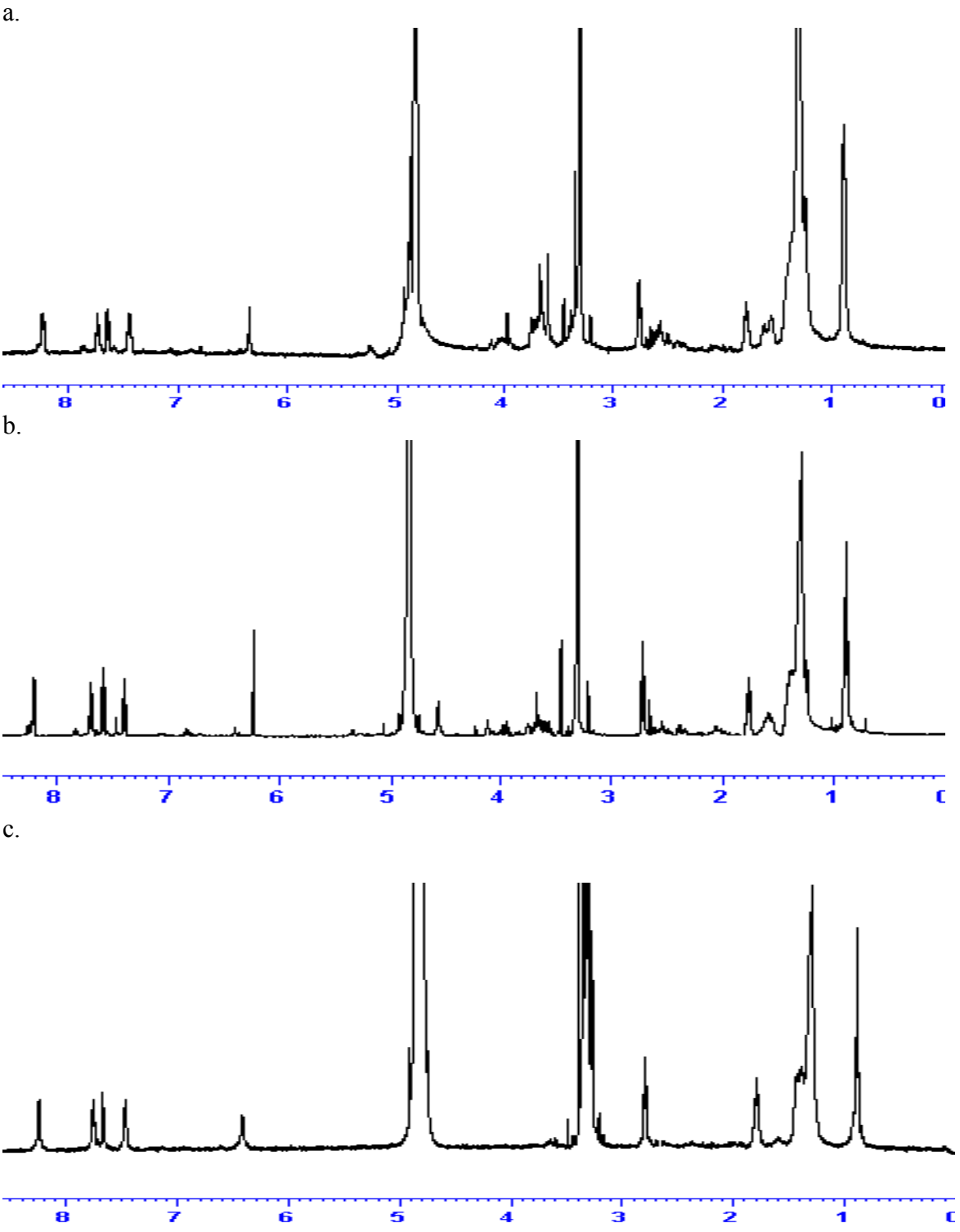

Figure 31. ^{1}H NMR spectra of 4-hydroxy-2-nonylquinoline (1) cleanup stages.
a.) *Pa*2P4-2-2-10
b.) *Pa*2P4-2-2-10-2
c.) *Pa*2P4-2-2-10-2-1

The cell signaling data also indicated that pyoluteorin can act as an autoinducer while inhibiting the growth of the assay strain. Pyoluteorin has previously been shown to repress *P. aeruginosa* gene expression of the antifungal metabolite 2,4-diacetylphloroglucinol (Schnider-Keel et al., 2000). This study reveals the possible role of pyoluteorin in the induction of the production of B-galactosidase in *P. aeruginosa*.

Prorocentrum species Isolates

Each DSP related compound tested in the bacterial cell-signaling bioassay, OA, DTX-1, and the diol ester mixture (30 μg each), demonstrated slight inhibition of the assay strain. The effect of *Pl*2E2-2, the DSP diol mixture, on B-galactosidase activity was 352 Miller Units (MU) compared with 405 MU for the control. Addition of OA (10) to the assay strain resulted in a response of 395 MU, while addition of DTX-1 (11) gave 362 MU compared with the the control (405 MU). Testing of larger quantities of each DSP related sample would generate data that could aid in determining the significance of these results.

A partially purified mixture from the ethyl acetate extract of *P. lima* cell-free culture media (8 L), demonstrated activity in the *P. aeruginosa* cell-signaling bioassay. LC/MS analysis of this extract indicated that no known autoinducers were present in the sample. A second extract of *P. lima* culture media (8 L) extract, also demonstrated activity in the *P. aeruginosa* cell-signaling bioassay, and once again no known autoinducers could be observed by LC/MS analysis.

DISCUSSION

DSP Toxins

Known DSP toxins include OA, DTX-1, and DTX-2. In this study, two new methyl derivatives of OA were detected, isolated and partially characterized from non-axenic cultures of a *P. lima* Gulf of Mexico isolate. These methyl derivatives of OA were present in minute quantities compared with OA and DTX-1, and identification is based primarily upon LC/MS data. LC/MS data has been used previously to identify trace amounts of the OA analogues DTX-2B and DTX-2C, isolated from mussels and *Dinophysis* species, respectively (James et al., 1997; Draisci et al., 1998). However, the substitution pattern of the methyl substituents could not be established.

In a separate study (Holmes et al., 1999), five methyl-OA derivatives were detected in extracts of the green mussel *Perna viridis* collected from the Johor Strait, Singapore, though they could be derivatives produced by the mussel itself. All reported isomers exhibited less polarity than DTX-1, eluting after the known toxin in reversed phase column chromatography (Holmes et al., 1999). The methyl OA derivatives in this study both elute prior to DTX-1 on a C_{18} column, demonstrating a higher polarity, more in keeping with the free acid structure. The isolation of more material of these derivatives is necessary to complete the structure elucidation.

Many diol esters of both OA and DTX-1 have been previously described (Hu et al., 1992). Generally speaking, the diol moiety contains seven to nine carbons with zero to two degrees of unsaturation (Hu et al., 1992). During this investigation, a new C_{10} diol ester of OA was also detected and partially characterized. The diol esters of DSP toxins are non-toxic *in vitro* but are toxic *in vivo* when the lipophilic diol ester is readily taken in

by cells and hydrolyzed to yield the free toxin (Windust et al., 1997; Wright unpublished data). The diol moiety of the OA C_{10} diol isolated in this study contains three degrees of unsaturation, arranged as a conjugated diene system with a third isolated double bond.

The discovery of the three new DSP compounds, present in minute quantities, was facilitated by the application of a new, efficient method developed during this investigation for the isolation of OA and its derivatives. Following detection of OA in *P. lima* cell-free culture media, a procedure was developed to induce the release of additional toxin to the media. Cultures were carefully decanted and the concentrated cells subjected to a freeze-thaw-sonicate routine. The concentrated cell mixture was allowed to sit overnight and filtered the next morning. The filtrate was applied to a conditioned C18 column. Following concentration of the organics from the media on a C_{18} column, and subsequent elution with a gradient of aqueous methanol, the only additional purification step necessary was reversed phase HPLC. Since the number of steps in a purification scheme is generally proportional to the recovery, fewer steps will generally result in a greater yield in less time. Similarly, this approach could result in an increased yield of minor components present in the concentrate to bring them above the detection limits of LC/MS and other spectroscopic techniques.

In addition to the discovery of new compounds, the purification of increased quantities of known DSP toxins is of value, since these compounds have not been chemically synthesized to date. Okadaic acid is expensive ($2200/mg) and other DSP toxins are currently unavailable for purchase. Ongoing research on marine toxins as well as protein phosphatases provides a continuous market for these toxins, and this rapid clean-up process could be useful in the commercial preparation of these compounds.

Cell-signaling

P. aeruginosa Isolates

$3OC_{12}HSL$ and C_4HSL are the two autoinducers primarily responsible for regulating the *P. aeruginosa* cell-signaling cascade and the expression of numerous antibiotics and virulence factors. Recently however, other secondary metabolites produced by the organism such as 2-heptyl-3-hydroxy-4-quinolone have been found to act as autoinducers (Pesci et al., 1999). In this study, no HSL autoinducers were observed, though a simple mixture containing 4-hydroxy-2-nonyl quinolone, in addition to small amounts of several other hydroxy-quinolines, exhibited autoinducer activity. Activity was lost, however, upon further purification of the individual components of the mixture. The possibility exists that the autoinducer activity exhibited by the mixture was generated by a compound present in minute amounts or with a weak chromophore, and therefore not collected during UV-DAD guided fractionation of the mixture.

Another possibility is that the autoinducer activity exhibited by the hydroxy-quinoline mixture is a result of synergy. Each mixture of hydroxy-quinolines tested in the cell-signaling assay exhibited significant autoinducer activity, while the pure compounds exhibited only minute activity. This hypothesis is not unprecedented, as the presence of signaling compounds that act together in optimal ratios has been demonstrated by pheromone mixtures produced by insects (Wu et al., 1998).

P. lima Isolates

The initiation of bloom formation and toxin production in dinoflagellates is of interest as a possible means of control over these harmful algal bloom events. The presence of a chemical signal that induces either bloom formation, toxin production, or

some other critical aspect of dinoflagellate existence would provide a target, that if successfully attacked, could render the toxic dinoflagellate benign, or at least reduce the impact of a bloom event.

A mixture extracted during this investigation from the cell-free culture media of *P. lima* exhibited autoinducer activity in the cell-signaling assay. Although final purification of the active component of the mixture was unsuccessful due to lack of sufficient material, activity was increased upon partial purification of the active component. The entire procedure was repeated with identical results, indicating that there is indeed a single autoinducer or mixture of compounds produced by *P. lima* that is responsible for inducing the production of B-galactosidase in the cell-signaling assay.

Components of the mixture demonstrating activity in the cell-signaling assay included DTX-1 and one of the new methylated OA derivatives. Purified DTX-1 exhibited no autoinducer activity in the bioassay used in this study, however an interesting observation was made regarding the proportion of the known toxins OA and DTX-1 present. DTX-1 was found to be more abundant than OA in extracts from the cell-free media, while OA was more abundant than DTX-1 in cell extracts. Preferential excretion of DTX-1 from the cells would explain this phenomenon, possibly indicating its role as a signaling compound. Testing DTX-1 in bioassays designed to measure a direct phenotypic response of *P. lima* would perhaps be more relevant in determining the effect of DTX-1 or other DSP compounds on gene expression and cell growth of *P. lima*.

The experiments presented in this study represent the first report of autoinducer activity exhibited by an extract of a unicellular eukaryotic photosynthetic microalgae. The growth of *P. lima* under non-axenic culture conditions allows for the possibility that

the active metabolite is produced by one of the associated bacteria or the dinoflagellate itself. Determination of the structure of this autoinducer would help in identifying the producer organism. This in turn would begin to address the many questions regarding the role of bacteria in the toxin production and bloom formation of toxic dinoflagellates, perhaps generating information on a new target for controlling *P. lima* bloom formation and toxin production.

LITERATURE CITED

Allen, N. E.; Nicas, T. I. (2003) Mechanism of action of oritavancin and related glycopeptide antibiotics. *FEMS Microbiology Reviews,* 26(5), 511-532.

Baden D.; Fleming L. E.; Bean J. A. (1995) Marine Toxins. *Handbook of Clinical Neurology: Intoxications of the Nervous System Part II. Natural Toxins and Drugs*. F.A. deWolff *ed*., Amsterdam: Elsevier Press, 141-175.

Baran, M.; Mazerski, J. (2002) Molecular modelling of membrane sterols with the use of the GROMOS 96 force field. *Chemistry and Physics of Lipids,* 120(1-2), 21-31.

Baumann, U.; Stocklossa, C.; Greiner, W.; von der Schulenburg, J. G.; von der Hardt, H. (2003) Cost of care and clinical condition in paediatric cystic fibrosis patients. *Journal of Cystic Fibrosis,* 2(2), 84-90.

Bloemberg, G. V.; Lugtenberg, B. J. J. (2001) Molecular basis of plant growth promotion and biocontrol by rhizobacteria. *Current Opinion in Plant Biology*, 4, 343-350.

Calfee, M. W.; Coleman, J. P.; Pesci, E. C. (2001) Interference with *Pseudomonas* quinolone signal synthesis inhibits virulence factor expression by *Pseudomonas aeruginosa*. *Microbiology*, 98(20),

Collier, D. N.; Anderson, L.; McKnight, S.; Noah, T. L.; Knowles, M.; Boucher, R.; Schwab, U.; Gilligan, P.; Pesci, E. C. (2002) A bacterial cell to cell signal in the lungs of cystic fibrosis patients. *FEMS Microbiology Letters*, 215, 41-46.

Contreras, B., et.al. (1997) Isolation, purification, and amino acid sequence of Lactobin A, one of the two bacteriocins produced by *Lactobacillus amylovorus* LMG P-13139. *Applied and Environmental Microbiology*, 63(1), 13-20.

DellaGreca, M.; Fiorentino, A.; Monaco, P.; Previtera, L.; Temussi, F. and Zarrelli, A. (2003) New dimeric phenanthrenoids from the rhizomes of *Juncus acutus*. Structure determination and antialgal activity, *Tetrahedron,* 59(13), 2317-2324.

De Souza, J. T.; Raaijmakers, J. M. (2003) Polymorphisms within the *prnD* and *pltC* genes from pyrrolnitrin and pyoluteorin-producing *Pseudomonas* and *Burkholderia* spp., *FEMS Microbiology Ecology,* 43(1), 21-34

Draisci, R.; Giannetti, L.; Lucentini, L.; Marchiafava, C.; James, K. J.; Bishop, A. G.; Healy, B. M.; Kelly, S. S. (1998) Isolation of a new okadaic acid analogue from phytoplankton implicated in diarrhetic shellfish poisoning, *Journal of Chromatography A,* 798 (1-2), 137-145.

Egan, S.; James, S.; Holmstrom, C.; and Kjelleberg, S. (2001) Inhibition of algal spore germination by the marine bacterium *Pseudoalteromonas tunicata*. *FEMS Microbiology*

Ecology, 35(1), 67-73.

El-Samerraie, F. T.; Mohammed, A. R.; Al-Mosawi, M. A.; Matloob, S. E. (1997) Treatment of *Pseudomonas* life threatening chronic suppurative otitis media by new conservative therapy: a prospective study 1993-1994. *Medical Journal of Islamic Academy of Sciences*, 10(4), 1-8.

Gerber, N. N. (1973) Microbial phenazines. Handbook of Microbiology, Volume III: Microbial Products, CRC Press, eds. Laskin, A. I.; Lechevalier, H. A., 329-332.

Habeck, M. (2003) Stop talking at the back. *Drug Discovery Today*, 8(7), 279-280.

Harvey, A. (2000) Strategies for discovering drugs from previously unexplored natural products. *Drug Discovery Today*, 5(7), 254-.

Hauksson, J. B.; Bergqvist, M. H. J.; Rilfors, L. (1995) Structure of digalactosyldiacylglycerol from oats. *Chemistry and Physics of Lipids*, 78, 97-102.

Hayamizu, K.; Yanagisawa, M.; Yamamoto, O. (2003) Integrated Spectral Data Base System for Organic Compounds, National Institute of Advanced Industrial Science and Technology, Tsukuba, Ibaraki, Japan. SDBSWeb:http://www.aist.go.jp/R10DB/SDBS

Henrickson, A. A. and Pawlik, J. R. (1995) A new antifouling assay method: results from field experiments using extracts of four marine organisms. *Journal of Experimental Marine Biology and Ecology*, 194(2), 157-165.

Hernandez, M. E.; Newman, D. K. (2001) Review: extracellular electron transfer. *Cell. Mol. Life Sci*., 58, 1-10.

Holden, M. T. G.; Chhabra, S. R.; de Nys, R.; Stead, P.; Bainton, N. J.; Hill, P. J.; Manefield, M.; Kumar, N.; Labatte, M.; England, D.; Rice, S.; Givskov, M.;Salmond, P. C.; Stewart, G. S. A. B.; Bycroft, B. W.; Kjelleberg, S.; Williams, P. (1999) Quorum-sensing cross talk: isolation and chemical characterization of cyclic dipeptides from *Pseudomonas aeruginosa* and other gram-negative bacteria. *Molecular Microbiology*, 33(6), 1254-1266.

Holmes, M. J.; Teo, S. L. M.; Lee, F. C.; Khoo, H. W. (1999) Persistent low concentrations of diarrhetic shelfish toxins in green mussels *Perna viridis* from the Johor Strait, Singapore: first record of diarrhetic shellfish toxins from South-East Asia. *Marine Ecology Progress Series*, 181, 257-268.

Holmstrom, C.; Egan, S.; Franks, A.; McCloy, S.; Kjelleberg, S. (2002) Antifouling activities expressed by marine surface associated *Pseudoalteromonas* species, *FEMS Microbiology Ecology,* 41(1), 47-58.

Hoyt, P.; Sizemore, R. (1982) Competitive dominance by a bacteriocin-producing *Vibrio harveyi* strain. *Applied and Environmental Microbiology*, 44(3), 653-658.

Hu, T.; Curtis, J. M.; Walter, J. A.; McLachlan, J. L.; Wright, J. L. C. (1995) Two new water soluble DSP toxin derivatives from *Prorocentrum maculosum*: Possible storage and excretion products of the dinoflagellate. *Tetrahedron Letters*, 36, 9273-9276.

Hu, T.; Curtis, J.M.; Walter, J. A.; Wright, J. L. C. (1994) Identification of DTX-4, a new water-soluble phosphatase inhibitor from the toxic dinoflagellate *Prorocentrum lima*. Journal of the Chemical Society, Chemical Communications, 597-599.

Hu, T.; deFreitas, A. S. W.; Doyle, J.; Jackson, D.; Marr, J.; Nixon, E.; Pleasance, S.; Quilliam, M. A.; Walter, J. A.; Wright, J. L. C. (1993) New dsp toxin derivatives isolated from toxic mussels and the dinoflagellates *Prorocentrum lima* and *Prorocentrum concavum*. *Toxic Phytoplankton Blooms in the Sea*, Elsevier Science Publishers B.V., 507-512.

Hu, T.; Marr, J.; deFreidas, A. S. W.; Quilliam, M. A.; Walter, J. A.; Wright, J. L. C. (1992) New diol esters isolated from cultures of the dinoflagellates Prorocentrum lima and Prorocentrum concavum. *Journal of Natural Products*, 55(11), 1631-1637.

James, K. J.; Carmody, E. P.; Gillman, M.; Kelly, S. S.; Draisci, R.; Lucentini, L.; Giannetti, L. (1997) Identification of a new diarrhoetic toxin in shellfish using liquid chromatography with fluorimetric and mass spectrometric detection, *Toxicon,* 35 (6), 973-978.

Jayatilake, G. S.; Thornton, M. P.; Leonard, A. P.; Grimwade, J. E.; Baker, B. J. (1996) Metabolites from an Antarctic sponge-associated bacterium, *Pseudomonas aeruginosa*. *Journal of Natural Products,* 59(3), 293-296.

Kerr, J. (2000) Phenazine pigments, antibiotics and virulence factors. *The Infectious Disease Review—microbes of man, animals and the environment*, 2(4), 184-194.

Klaenhammer, T. (1993) Genetics of bacteriocins produced by lactic acid bacteria. *FEMS Microbiology Reviews*, 12, 39-86.

Kuklev, D. V.; Aizdaicher, N. A.; Imbs, A. B.; Bezuglov, V. V.; Latyshev, N. A. (1992) All-cis-3,6,9,12,15-octadecapentaenoic acid from the unicellular alga Gymnodinium kowalevskii. Phytochemistry, 31(7), 2401-2403.

Landsberg, J. H.; Balazs, G. H.; Steidinger, K. A.; Baden, D. G.; Work, T. M.; Russell, D. J. (1999) The potential role of natural tumor promoters in marine turtle fibropapillomatosis. *Journal of Aquatic Animal Health,* 11, 199-210.

Leblond, J. D.; Chapman, P. J. (2000) Lipid class distribution of highly unsaturated long chain fatty acids in marine dinoflagellates. *Journal of Phycology*, 36, 1103-1108.

Lewenza, S.; Visser, M. B.; Sokol, P. A. (2002) Interspecies communication between *Burkholderia cepacia* and *Pseudomonas aeruginosa*. *Canadian Journal of Microbiology*, 48, 707-716.

Li, Z.; Wang, X.; Guo, Y; Zhao, J. (1995) Inhibitory action of metabolites of *Pseudomonas aeruginosa* against gram-negative bacteria. *Kansenshogaku Zasshi. The Journal of the Japanese Association for Infectious Diseases*, 69(8), 924-927.

Macpherson, G. R.; Burton, I. W.; LeBlanc, P.; Walter, J. A.; Wright, J. L. C. (2003) Studies of the biosynthesis of DTX-5a and DTX-5b by the dinoflagellate *Prorocentrum maculosum*: Regiospecificity of the putative Baeyer-Villigerase and insertion of a single amino acid in a polyketide chain. *Journal of Organic Chemistry,* 68(5),1659-1664.

Mayr-Harting, A.; Hedges, A.; Berkeley, R. (1972) Methods for studying bacteriocins. *Methods in Microbiology*, 315-422.

McKnight, S. L.; Iglewski, B. H.; and Pesci, E. C. (2000) The *Pseudomonas* quinolone signal regulates rhl quorum sensing in *Pseudomonas aeruginosa*. *Journal of Bacteriology*, 182(10), 2702-2708.

Metcalf, J. S.; Lindsay, J.; Beattie, K. A.; Birmingham, S.; Saker, M. L.; Torokne, A. K.; Codd, G. A. (2002) Toxicity of cylindrospermopsin to the brine shrimp *Artemia salina*: comparisons with protein synthesis inhibitors and microcystins. *Toxicon,* 40(8), 1115-1120.

Michel-Briand, Y.; Baysee, C. (2002) The pyocins of *Pseudomonas aeruginosa*. *Biochimie*, 84(5-6), 499-510.

Olsen, J. A.; Severinsen, R.; Rasmussen, T. B.; Hentzer, M.; Givskov, M.; Nielsen, J. (2002) Synthesis of new 3- and 4-substituted analogues of acyl homoserine lactone quorum sensing autoinducers. *Bioorganic and Medicinal Chemistry Letters*, 12, 325-328.

Parret, A.; De Mot, R. (2002) Bacteria killing their own kind: novel bacteriocins of *Pseudomonas* and other g-proteobacteria. *Trends in Microbiology*, 10(3), 107-112.

Pawlik, J. R.; Burch, M. T.; Fenical, W. (1987) Patterns of chemical defense among Caribbean gorgonian corals: a preliminary survey. *Journal of Experimental Marine Biology and Ecology*, 108(1), 55-66.

Pesci, E. C.; Milbank, J. B.; Pearson, J. P.; McKnight, S.; Kende, A. S.; Greenberg, E. P.; Inglewski, B. H. (1999) Quinolone signaling in the cell-to-cell communication system of *Pseudomonas aeruginosa*. *Proceedings of the National Academy of Sciences*, 96, 11229-11234.

Piva, A.; Headon, D. (1994) Pediocin A, a bacteriocin produced by *Pediococcus pentosaceus* FBB 61. *Microbiology*, 140, 697-702.

Prokic, E.; Brummer, F.; Brigge, T.; Gortz, H. D.; Gerdts, G.; Schutt, C.; Elbrachter, M.; Muller, W. E. G. (1998) Bacteria of the genus *Roseobacter* associated with the toxic dinoflagellate *Prorocentrum lima*. *Protist*, 148, 347-357.

Quilliam, M. A.; Wright, J. L. C. (1995) Methods for diarrhetic shellfish poisons. *Intergovernmental Oceanographic Commission (of UNESCO): Manual on Harmful Marine Microalgae,* Hallegraeff, G.M., Anderson, D. M., Cembella, A. D., eds., United NationsEducational, Scientific and Cultural Organization, 95-112.

Raaijmakers, J.; Weller, D.; Thomashow, L. (1997) Frequency of antibiotic-producing *Pseudomonas* spp. in natural environments. *Applied and Environmental Microbiology*, 63(3), 881-887.

Rai, A. K.; Rai, S. B.; Rai, D. K. (2003) Quantum chemical studies on the conformational structure of bacterial peptidoglycans and action of penicillin on cell wall. *Journal of Molecular Structure: THEOCHEM,* 626(1-3), 53-61.

Rasmussen, T. B.; Manefield, M.; Anderson, J. B.; Eberl, L.; Anthoni, U.; Christopherson, C.; Steinberg, P.; Kjelleberg, S.; Givskov, M. (2000) How *Delisea pulchra* furanones affect quorum sensing and swarming motility in Serratia liquefaciens MG1. *Microbiology*, 146, 3237-3244.

Rausch de Traubenberg, C.; Soyer-Gobillard, M.; Geraud, M.; Albert, M. (1995) The toxic dinoflagellate Prorocentrum lima and its associated bacteria: II. Immunolocation of okadaic acid in axenic and non-axenic cultures. *European Journal of Protistology*, 31, 383-388.

Rotani, J. F.; Volkman, J. K. (2003) Phytol degradation products as biogeochemical tracers in aquatic environments. *Organic Geochemistry*, 34(1), 1-35.

Royt, P. W.; Honeychuck, R. V.; Ravich, V.; Ponnaluri, P.; Pannell, L. K.; Buyer, J. S.; Chandhoke, V.; Stalick, W. M.; DeSesso, L. C.; Donohue, S.; Ghei, R.; Relyea, J. D.; Ruiz, R. (2001) 4-Hydroxy-2-nonylquinoline: a novel iron chelator isolated from a bacterial cell membrane. *Bioorganic Chemistry*, 29, 387-397.

Sakai, R.; Rinehart, K. L. (1995) A new polyether acid from a cold water marine sponge, a *Phakellia* species. *Journal of Natural Products*, 58(5), 773 –777.

Schlünzen, F.; Harms, J. M.; Franceschi, F.; Hansen, H. A. S.; Bartels, H.; Zarivach, R.: Yonath, A. (2003) Structural Basis for the Antibiotic Activity of Ketolides and Azalides, *Structure,* 11(3), 329-338.

Schnider-Keel, U.; Seematter, A.; Maurhofer, M.; Blumer, C.; Duffy, B.; Gigot-Bonnefoy, C.; Reimmann, C.; Notz, R.; Defago, G.; Haas, D.; Keel, C. (2000) Autoinduction of 2,4-diacetylphloroglucinol biosynthesis in the biocontrol agent *Pseudomonas fluorescens* CHA0 and repression by the bacterial metabolites salicylate and pyoluteorin. *Journal of Bacteriology*, 182(5), 1215-1225.

Smith, K. M.; Bu, Y.; Suga, H. (2003) Induction and inhibition of *Pseudomonas aeruginosa* quorum sensing by synthetic autoinducer analogs. *Chemistry and Biology*, 10, 81-89.

Smith, R. S.; Inglewski, B. H. (2003) P. aeruginosa quorum sensing systems and virulence. *Current Opinion in Microbiology*, 6(1), 56-60.

Stead, P.; Rudd, B. A.; Bradshaw, H.; Noble, D.; Dawson, M. J. (1996) Induction of phenazine biosynthesis in cultures of *Pseudomonas aeruginosa* by L-N-(3-oxohexanoyl) homoserine lactone. *FEMS Microbiology Letters*, 140(1), 15-22.

Tachibana, K.; Sheuer, P. (1981) Okadaic acid, a cytotoxic polyether from two marine sponges of the genus *Halichondria*. *Journal of the American Chemical Society*, 103, 2469-2471.

Taylor, G.; Machan, Z.; Mehmet, S.; Cole, P. J.; Wilson, R. (1995) Rapid identification of 4-hydroxy-2-alkylquinolines produced by *Pseudomonas aeruginosa* using gas chromatography-electron-capture mass spectrometry. *Journal of Chromatography B*, 664, 458-462.

Van Delden, C. and Iglewski, B. H. (1998) Cell-to-cell signaling and *Pseudomonas aeruginosa* infections. *Emerging Infectious Diseases*, 4(4), 1-13.

Windust, A. J.; Quillium, M. A.; Wright, J. L. C.; McLachlan, J. L. (1997) Comparative toxicity of the diarrhetic shellfish poisons, okadaic acid, okadaic acid diol-ester, and dinophysistoxin-4, to the diatom *Thalassiosira weissflogii*. *Toxicon*, 35(11), 1591-1603.

Wright, J. L. C.; Hu, T.; McLachlan, J. L.; Needham, J.; Walter, J. A. (1996) Biosynthesis of DTX-4: Confirmation of a polyketide pathway, proof of a Baeyer-Villiger oxidation step and evidence for an unusual carbon deletion process. *Journal of the American Chemical Society*, 36, 8757-8758.

Wright, J. L. C. (2002) Attack and defend: the function and evolution of bioactive or toxic metabolites *Xth International Conference on Harmful Algal Blooms Book of Abstracts*, 1.

Wu, W.; Zhu, J.; Millar, J.; Lofstedt, C. (1998) A comparative study of sex pheromone biosynthesis in two strains of the turnip moth, *Agrotis segetum*, producing different ratios of sex pheromone components, *Insect Biochemistry and Molecular Biology*, 28 (11), 895-900.

Yasumoto, T.; Murata, M.; Oshima, Y.; Sano, M.; Matsumoto, G. K.; Clardy, J. (1985) Diarrhetic Shellfish Toxins. *Tetrahedron*, 41(6), 1019-1025.